2011

CHARACTERIZATION OF HtsA, THE FERRIC-STAPHYLOFERRIN A-BINDING PROTEIN IN STAPHYLOCOCCUS AUREUS

John D.E. Cooper

CHARACTERIZATION OF HtsA, THE FERRIC-STAPHYLOFERRIN A-BINDING PROTEIN IN *STAPHYLOCOCCUS AUREUS*

(Spine title: Staphyloferrin A-mediated Iron Uptake in *S. aureus*)

(Thesis format: Monograph)

by

John D.E. Cooper

Graduate Program in Microbiology and Immunology

A thesis submitted in partial fulfillment
of the requirements for the degree of
Master of Science

The School of Graduate and Postdoctoral Studies
The University of Western Ontario
London, Ontario, Canada

THE UNIVERSITY OF WESTERN ONTARIO
SCHOOL OF GRADUATE AND POSTDOCTORAL STUDIES

CERTIFICATE OF EXAMINATION

Supervisor	Examiners
Dr. David Heinrichs	Dr. John McCormick
Supervisory Committee	Dr. Wayne Miller
Dr. Carole Creuzenet	Dr. Gilles Lajoie
Dr. Martin McGavin	

The thesis by

John D.E. Cooper

entitled:

Characterization Staphyloferrin A-Mediated Iron Uptake in *Staphylococcus aureus*

is accepted in partial fulfillment of the
requirements for the degree of

Master of Science

Date

Chair of the Thesis Examination Board

Abstract

The frequent human pathogen *Staphylococcus aureus* requires a sufficient source of iron to proliferate and, thus, to sustain an infection of a mammalian host. However, the free iron concentration in the host is insufficient for bacterial growth without use of specialized uptake mechanisms. To overcome this, *S. aureus* utilizes multiple systems to scavenge host iron. One such strategy that *S. aureus* employs is the use of siderophores: secreted, small-molecular-weight, high-affinity iron chelators. *S. aureus* synthesizes and secretes two anionic α-hydroxycarboxylate siderophores, staphyloferrin A (SA) and staphyloferrin B (SB). Fe-SA and Fe-SB complexes are transported into the cell through the highly specific ABC-type transporters HtsABC and SirABC, respectively. The crystal structures of HtsA, the SA receptor, have been solved for both SA bound and unbound forms. Structural data indicate that HtsA has a unique positively charged binding pocket and many charged residues form contacts with the anionic siderophore including R86, R104, R126, K203, H209, and Y239. Their contribution to productive binding and transport is currently unknown. To investigate the role of each residue found to interact with SA, site-directed mutagenesis was used to substitute each interacting residue with either alanine or an amino acid with more conserved properties. Fluorescence titrations of SA, produced and purified *in vitro*, with wild-type (WT) or mutant rHtsA were used to determine the effect that each substitution had on the binding affinity of HtsA for SA. Growth curves and disk-diffusion assays were completed on strains expressing mutated or WT HtsA to determine the biological significance of each mutation under SA-dependant growth conditions. These studies have confirmed significant roles in SA binding and transport

for HtsA residues R104, R126, and H209, strengthening the conclusions drawn from the HtsA crystal structure and providing new insight into the mechanism of SA-dependant iron uptake in *S. aureus*.

Key Words: *Staphylococcus aureus*, ABC-transporters, HtsABC, iron transport, siderophores, staphyloferrin A

Co-authorship

Some of the work presented in this thesis was contributed by Dr. Michael Murphy and Dr. Jason Grigg. They solved the apo and holo crystal structures of rHtsA and contributed figures for the HtsA binding pocket and conformational changes.

Acknowledgements

First and foremost I must thank my supervisor, Dr. David Heinrichs, who was always enthusiastic about my research and constantly available to help, even making an extra effort to discuss my project when I let our weekly meetings become not so weekly. His support extended beyond lab hours, coming in early Sunday mornings to hear me rehearse presentations he had already sat through. Also, with his reference letters and support I received major scholarships and recently, acceptance into medical school.

Secondly, I would like to thank all the members of the Heinrichs lab. In one way or another, they helped me attain my research goals. I must give special thanks to Enrique who provided my initial training and Johnson who was a huge help with the dreaded HPLC and friendly but still finicky FPLC. Lastly, Fred Beasley, the senior Ph.D., was the go to guy for the lab. Although it was "just like TAing", he helped answer many of my questions. Also, I thank Catherine and Cristina for taking care of the ordering.

In addition, I would like to thank my collaborators at UBC, Dr. Murphy and Jason Grigg, for their work on the HtsA crystal structures. I must also thank Mike Tiedemann and the Stillman Laboratory for their expertise and help with AAS. I was also very fortunate to be trained by Leanne Briere in the bimolecular structures and conformations facility. She was extremely knowledgeable and a great instructor for the spectrofluorometer.

I'd like to thank Suya and Liliana for their time and the LC/MS chromatographs and CD spectras, respectively. I am grateful for the advice and guidance of my advisory committee, Dr. Creuzenet and Dr. McGavin and I would also like to thank the

Microbiology departmental office staff, especially Jennifer Brace, for going out of her way to make my degree as comfortable as possible.

Lastly, I must thank my family and my amazing fiancé Jenn. They were extremely supportive and helped me much more than they know. Special thanks are owed to Jenn, as she listened to countless presentations and edited many of my applications (and there were many).

Table of Contents

List of Tables

List of Figures

List of Abbreviations

ABC	ATP-binding cassette
Agr	accessory gene regulator
BPD	binding-protein dependant
CA	community acquired
CoNS	coagulase-negative staphylococci
CoPS	coagulase-positive staphylococci
Da	Dalton
DAPA	L-2,-3-diamino-propionic acid
DNA	deoxyribonucleic acid
ECM	extracellular matrix
EDA	ethyldiamine
EDDHA	ethlylene diamine-di(*o*-hydroxyphenol acetic acid)
EDTA	ethylenediaminetetra-acetic acid
Em	erythromycin
Fe	iron
Fur	ferric uptake regulator
HTP	heme transport protein
H-bond	Hydrogen-bond
IgG	immunoglobulin
IM	inner membrane
Isd	iron-regulated surface determinant

K_d	dissociation constant
Km	kanamycin
LB	Luria-Bertani broth
Lf	lactoferrin
M	molar
Mb	megabase
Mg	magnesium
MGE	mobile genetic element
MSCRAMM	microbial surface components recognizing adhesive matrix molecules
MRSA	methicillin resistant *Staphylococcus aureus*
NIS	nonribosomal peptide synthesis-independent
NRPS	nonribosomal peptide synthesis
mL	milliliter
mM	millimolar
OD	optical density
OM	outer membrane
PBP	periplasmic binding protein
PCR	polymerase chain reaction
PLP	pyridoxal-5'-phosphate
PVL	Panton-Valentine Leukocidin
SA	staphyloferrin A
SAgs	superantigens
SarA	staphylococcal accessory regulator

SB	staphyloferrin B
SDS	sodium dodecyl sulphate
sp	species
Spa	Protein A
TAE	Tris-acetate EDTA
TBE	Tris-borate EDTA
Tc	tetracycline
TCRS	two component regulatory systems
Tf	transferrin
TMS	Tris-minimal succinate
TSB	tryptic soy broth
VRSA	vancomycin-resistant *S. aureus*
WT	wild-type
α-KG	α-ketoglutarate
μg	microgram
μL	microliter
μm	micrometer

Chapter 1 - Introduction

1.1. Staphylococci

1.1.1. Staphylococcus genus

Staphylococcus is derived from the Greek work *staphylé* which means "bunch of grapes", which describes their characteristic grape-like appearance when observed under a microscope (30). They belong to the family Staphylococcaceae which includes *Jeotgalicoccus*, *Micrococcus*, *Nosocomicoccus*, and *Salinoccus*. *Staphylococci* are spherical (approximately 1 μm in diameter), Gram-positive, facultative-anaerobes, that are non-motile and non-spore-forming. Depending on growth conditions, they can be found alone, in pairs, strings, or in clusters because their cell division occurs in more than one plane. They tend to form capsules *in vivo*, however, they produce little to no capsule when grown under standard laboratory conditions (105). They have a thick cell wall that consists of peptidoglycan with glycine cross-links, and wall teichoic acids and lipoteichoic acids (30).

1.1.2. *Staphylococcus aureus*

Staphylococcus aureus is a commensal and a pathogen. It produces a yellow carotenoid pigment, staphyloxanthin, distinguishing it from other staphylococci (123). *S. aureus* is one of few coagulase-positive staphylococci (CoPS) that harbour the gene encoding coagulase in their genome. The enzyme coagulase interacts with host factors in serum to clot blood, which may aid in immune evasion (126). *S. aureus* is the best studied species of staphylococci however, some notable coagulase-negative staphylococci (CoNS) include *S. saprophyticus*, *S. haemolyticus*, and *S. epidermidis* (72).

One of *S. aureus*' ecological niches is the anterior nares of humans. Approximately 20-30% of the population are persistent *S. aureus* carriers, and an additional 30% are intermittent carriers (152). More than eighty strains of *S. aureus* and 6 CoNS strains have had their complete genome sequenced. *S. aureus* genomes range from roughly 2.8 to 2.9Mbp and have an average G + C mol % content of 33% (69).

1.1.3. *S. aureus* pathogenesis

S. aureus is a significant human pathogen and is frequently responsible for blood, skin, soft tissue, and lower respiratory tract infections in North America and Europe (38). It is also the leading cause of nosocomial infections in the United States (140) and community-acquired (CA) infections are becoming increasingly prevalent (77). Furthermore, the CA strains tend to be more invasive than the traditional hospital acquired strains (79). *S. aureus* can infect multiple host tissue environments and cause mild infections including impetigo, pimples, boils, and food poisoning to more severe infections including toxic shock syndrome, osteomyelitis, pneumonia, necrotizing fasciitis, bacteraemia, sepsis, and staphylococcal scalded skin syndrome (150).

1.1.4. *S. aureus* virulence factors

The ability of *S. aureus* to produce productive infections in many different host tissue environments is largely due to its enormous repertoire of virulence factors. *S. aureus* encodes both structural and secreted virulence factors and many of them are encoded on mobile genetic elements (MGEs). Through transfer of genetic information, the MGEs increase the heterogeneity of *S. aureus* virulence factors and resistance determinants (95). Antibiotic resistance will be discussed in greater detail below. Many types of MGEs are found in *S. aureus* including plasmids, transposons, insertion sequences, bacteriophages, pathogenicity islands, and staphylococcal cassette chromosomes. Most staphylococcal MGEs are regulated by core genome global regulators allowing for careful regulation of virulence factor expression (37).

Adhesion of *S. aureus* to host molecules is achieved through microbial surface components recognizing adhesive matrix molecules (MSCRAMMs) (111). The MSCRAMM family of proteins includes a fibronectin-binding protein (FnBPA), a collagen-binding protein (Cna), clumping factor A (ClfA), and a fibrinogen-binding protein (142, 111), among others. Other surface proteins include protein A (Spa), which binds the Fc domain of immunoglobulin G (IgG), aiding immune evasion (142). It can also mediate attachment to host von Willebrand factor, a blood glycoprotein involved in hemostasis (63). *S. aureus* also has an elastin binding protein (EbpS) and can bind other host plasma and extra-cellular matrix (ECM) components, however, the mechanisms remain unclear.

Different strains of *S. aureus* have the ability to secrete a large variety of virulence factors, including exoenzymes such as proteases, lipases, and nucleases, and exotoxins, including α, β, γ, and δ toxins, Panton-Valentine Leukocidin (PVL), superantigens (SAgs), and superantigen-like proteins, and exfoliative toxins A and B. Collectively, these factors function to provide nutrients, modulate host immune mechanisms and damage tissues (36).

Regulation of staphylococcal virulence factors is essential for maintaining productive infections. Two global regulator families are responsible for proper virulence factor regulation. They are two component regulatory systems (TCRS) and the staphylococcal accessory regulator (SarA) protein family (16). Of 16 known *S. aureus* TCRSs the most notable system involved in pathogenesis is the accessory gene regulator (*agr*) quorum sensing system (22). The *agr* system is cell density dependant and at elevated cellular densities, such as those during post-exponential growth phase, the *agr* system increases secreted toxin production and decreases surface protein expression (148, 107). Additional TCRSs involved in *S. aureus* pathogenesis include SaeRS, (55, 56), ArlRS (48, 49), and SrrAB (154).

The SarA protein family consists of DNA-binding proteins that directly or indirectly regulate at least 120 staphylococcal genes. Furthermore, it has been demonstrated that SarA is required for the complete activation of *agr* expression (21). SarA levels are highest during the late exponential phase of growth leading to the highest expression levels of the fibronectin and fibrinogen binding protein adhesins and toxins that promote dispersion (22). Additionally, it represses Spa and protease

expression (22). SarA elicits its effects directly by binding gene promoters, indirectly via downstream effects of regulons, or by stabilizing mRNA transcripts (22, 121).

1.1.5. *S. aureus* antibiotic resistance

S. aureus antibiotic resistance is a growing problem in nosocomial and CA infections. *S. aureus* develop resistance through a number of mechanisms. One of the first mechanisms identified was the production of a secreted penicillinase (BlaZ), which hydrolytically cleaves β-lactams (19). More recently, methicillin resistant *Staphylococcus aureus* (MRSA), which is propagated on MGEs (SCC*mec*), have become a growing concern (61). There are currently 8 SCC*mec* types, abbreviated I-VIII, which have been subdivided into 5 classes. Each class contains *mecA*, which encodes a low-affinity penicillin binding protein (PBP2a) that prevents binding of methicillin or other ß–lactam antibiotics (20).

In addition to *mecA*, other antibiotic resistance determinants are frequently associated with the SSCmec MGEs. These include resistance to erythromycin (*ermB*, *ermC*), spectinomycin (*aad9* or *spc*), tetracycline (*tet*), aminoglycosides (*aacA-aphD*), bleomycin (*ble*), and tobramycin (*ant4'*) (36). More recently, staphylococci have acquired vancomycin resistance from enterococci resulting in vancomycin-resistant *S. aureus* (VRSA) (151). Vancomycin resistance is mediated by VanA and VanH which synthesize a D-Ala-D-Lac precursor that has reduced affinity for glycopeptide antibiotics (89). In addition, VanX mediates the elimination of the D-Ala-D-Ala peptides that are susceptible to glycopeptide antibiotics, thus eliminating the drug targets (88).

Consequently, there is a drastic need for the identification of new therapeutic targets, such as the interruption of access to the essential nutrient iron.

1.2. Iron

Iron is an essential nutrient for almost all living organisms. The only known exceptions are some lactobacilli (1) and spirochaetes (116). Iron exists predominantly in two oxidative states, ferrous Fe^{2+}(FeII) or ferric Fe^{3+}(FeIII). The ability to transition between those oxidative states is essential for the catalytic roles that iron has in most organisms (114). Indeed, iron can be found in essential enzymes involved in the electron transport chain, carbon utilization, DNA replication, and oxygen metabolism (4).

1.3. Iron solubility

Although iron constitutes a significant proportion of the earth, the vast majority of it is unavailable for biological activity. This is largely due to the rapid oxidation of ferrous iron by molecular oxygen (104). The resulting iron-hydroxide precipitates are stable and extremely insoluble culminating into a final free iron concentration of approximately 10^{-9} M at a neutral pH (118).

1.4. Iron in the human host

Further evidence of iron's biological importance is demonstrated by a human host's non-specific defence mechanisms that function to limit iron availability. Most iron is found intracellulary complexed to haemoglobin (76%) or ferritin (23%) (109). Additionally, extracellular iron-binding proteins, especially transferrin and lactoferrin,

further depress the free iron available leading to essentially no free iron in the host (118). The abundance of iron binding proteins involved in proper iron homeostasis and maintenance of low extracellular levels within a human host highlight iron's importance. Heightened iron levels can bolster infections, as patients with thalassemia or other forms of iron overload are more susceptible to infections (149), or it can lead to the production of free radicals under aerobic conditions. However, insufficient iron has severe consequences on essential cellular processes including oxygen transport, electron transport, and RNA and DNA synthesis. Furthermore, during an infection iron is actively sequestered by the reticuloendothelial system (90). Therefore, iron limitation in the human host is a significant obstacle that microorganisms must overcome in order to sustain infections.

1.5. Regulation of iron uptake

Proper organization and regulation of iron transport is an essential process. The most important iron-regulatory protein is the ferric uptake regulator (Fur), an iron-dependant repressor protein found in both Gram-negative and Gram-positive bacteria, including *S. aureus* (146), and more than 60 homologues have been found (15). Other iron-responsive repressor proteins have been identified, such as RirA-type regulatory proteins; however, Fur is by far the most important (139, 146). Under physiologically adequate levels of cellular iron Fur binds ferrous iron. Dimeric Fur-Fe(II) complexes then bind specific DNA regulatory sequences at Fur boxes, a 19-bp inverted repeat, located within the operator region of target genes and repress transcription (62, 158). Fur regulates more than 90 *E. coli* genes in this manner (139). Additionally, it has been

demonstrated that Fur can also indirectly activate genes through repression of small RNA silencing molecules (98) and directly upregulate other genes (35).

1.6. Bacterial iron acquisition strategies

Many organisms have developed means of scavenging human host iron. Due to iron's strict limitation, multiple strategies are frequently employed by successful pathogens. These systems work in concert to access and internalize host iron sources. For instance, some bacteria secrete toxins that lyse host cells in order to gain access to intracellular iron stores. Additionally, other systems can recognize host extracellular iron containing sources.

1.6.1. Ferric reductases

One mechanism that bacteria use to acquire host iron is to reduce highly insoluble ferric iron (10^{-18} M) to much more soluble ferrous iron (0.1 M) at a pH of 7.0 (4). *Listeria monocytogenes* has two of the best-characterized examples of ferric reductases. One is membrane-bound with a broad range of activity and the other is secreted and can reduce and remove iron from transferrin (28). Ferric reductase activity has now been shown in a number of bacterial (46), fungal (43), and plant species (44). Additionally, some organisms have a specific transport system for ferrous iron. For example, the *feo* system which was first identified in *E. coli*, is also present in *S. enterica* (11) and *H. pylori*, other colonizers of the human intestinal tract and stomach, respectively. It is anaerobically induced where conditions are more permissive for ferrous iron (76). A homologous system has also been identified in *S. aureus* (65).

1.6.2. Host iron-binding protein receptors

Some bacteria encode surface receptors that specifically recognize human host iron-binding glycoproteins as an iron source. *Neisseria gonorrhoeae* has two transferrin (Tf)-binding proteins, TbpA and TbpB (130), and two lactoferrin (Lf)-binding proteins that form Tf and Lf receptors on its cell surface (131). Other human pathogens, such as *Haemophilus influenzae,* have similar receptors (132). Both receptors bind Tf or Lf and remove iron for internalization without transporting the glycoproteins across the outer membrane (OM). These OM receptors have a β-barrel structure similar to porins however, an N-terminal globular domain prevents free diffusion of substrates into the periplasm. Instead, transport is dependent on TonB-ExbB-ExbD, an inner membrane embedded protein complex that interacts with a TonB box within the N-terminal globular domain of the OM receptors in order to facilitate transport (13). Iron is then bound by periplasmic substrate binding proteins which deliver the cargo to inner membrane ABC transporters which shuttle the cargo through the inner membrane (IM) in an ATP-consuming fashion (3).

1.6.3. Heme iron acquisition

Heme is a protoporphyrin ring with a centrally located iron atom. It is a hydrophobic prosthetic group found in many proteins and it is the most abundant potential iron source in the human host (109). It is found primarily intracellulary, however, following lysis of erythrocytes it is released into the extracellular milieu (115). In order to prevent damage from reactive heme molecules, it is quickly sequestered by hemopexin (73), lipoprotein (101), haemosiderin (71), or haptoglobin (53). Host macrophages will then internalize and clear the haptoglobin-hemoglobin or hemopexin-heme complexes, protecting the host from damage and limiting bacterial heme access (83). Under physiological conditions this highly efficient process reduces heme concentrations beneath detection limits in human serum (115). However, during an infection many bacteria, including *S. aureus*, secrete haemolysins that lyse erythrocytes and elevate the extracellular heme concentration (8). Several Gram-positive and Gram-negative bacterial systems have been identified that use heme as an iron source. Indeed, there are three types of heme transport systems that can obtain heme from host sources including hemopexin, haemoglobin, heme-albumin, and haemoglobin-haptoglobin (145).

1.6.3.1. Direct heme uptake systems

Direct heme uptake systems have been identified in Gram-negative and Gram-positive bacteria. In Gram-negative bacteria, heme is bound at the outer membrane and transported into the periplasm in a TonB-dependant fashion. It is then complexed to a heme transport protein (HTP) and shuttled into an ABC-transporter for internalization

into the cytosol (145). The *Pseudomonas aeruginosa phuR-phuSTUVW* is an example of a direct heme uptake system that contains an outer membrane receptor (PhuR), an HTP (PhuS), an ABC-transporter (PhuUVW), and a cytosolic protein (PhuS) (108). Similar systems are utilized by several other Gram-negative pathogens including *Yersinia pestis*, *Campylobacter jejuni*, and *E. coli* (102, 144, 147). There are fewer well-described heme transport systems in Gram-positive bacteria. *S. aureus* encodes an iron-regulated surface determinate system (Isd) that is composed of four cell wall-anchored proteins (IsdABCH), an ABC transporter (IsdDEF), and two heme oxygenases (IsdGH) (120). The surface proteins, IsdB and IsdH, bind haemoglobin or haemoglobin-haptoglobin (41) from which IsdA extracts heme and passes it to IsdC. Heme is then shuttled to IsdDEF which transports it across the cell membrane into the cytoplasm (106). The heme oxygenases then extract the iron for incorporation into proteins or storage (99, 120). The Isd locus is also found in other Gram-positive pathogens (145) however, *Corynebacterium* spp. and *Streptococcus* spp. use a direct heme uptake system that is distinct from Isd (2, 157). In *C. diptheriae*, *htaCA hmuTUV-htaB* encodes two heme receptors (HtaA & HtaB), a heme binding protein (HmuT) and an ABC-transporter (HmuUV) that internalizes the heme (2).

1.6.3.2. Hemophores

Both Gram-positive and Gram-negative hemophores have been identified. A hemophore is a secreted heme-binding protein that scavenges heme and is then recognized by a surface receptor that mediates heme uptake. Two Gram-negative hemophore systems have been characterized (145). The HasA hemophore system consists of a hemophore (HasA), an exporter (HasDEF), a receptor (HasR), two regulatory proteins (HasI and HasS) (52, 124) and is TonB- or the TonB homolog, HasB-dependant (110). This system has been identified in *Serratia marcescens*, *P. aeruginosa*, *P. fluorescens*, and *Y. pestis* (74, 91, 125). The HxuA hemophore system has only been identified in *Haemoplilus influenzae* type b and it consists of a hemophore (HxuA) that binds heme-hemopexin complexes, an exporter (HxuB), and a receptor (possibly HxuC) (26). *Bacillus anthracis* encodes the only known Gram-positive hemophores, IsdX1 and IsdX2. The hemophores are unique components of an Isd heme uptake system that is similar to but distinct from the *S. aureus* Isd (51). IsdX1 can remove heme from haemoglobin before passing it to IsdX2 or IsdC, which then transports heme into the cell through the Isd system (47).

1.6.4. Siderophores

Another common iron acquisition strategy that is utilized by an large number of bacteria is siderophores. A siderophore is a secreted, small (500-1500 Da), high-affinity Fe(III) chelator. There is an incredible diversity of siderophore structures and origins with more then 500 currently identified and structural information for more than half of them (65). Siderophores have been identified in plants (44), fungi (45), and microorganisms (50).

1.6.4.1. Siderophore biosynthesis

There are two classes of siderophore biosynthesis: nonribosomal peptide synthesis (NRPS) and nonribosomal peptide synthesis-independent (NIS) (18). NRPS synthesis occurs in a step-by-step process, usually through the addition of amino acids or their derivatives to a proteinaceous backbone by a large modular multienzyme (29). These complexes are not limited to the production of siderophores but are also responsible for the synthesis of most microbial peptide secondary metabolites including some antibiotics such as penicillin (129) and vancomycin (141). Some notable NRPS siderophores include enterobactin and yersiniabactin (119). NIS pathways usually rely on multiple synthetases that combine dicarboxcylic acids with diamines, alcohols, and amino alcohols (18). The best-known example of an NIS siderophore is aerobactin, assembled by two enzymatic synthetases (34). Interestingly, the siderophore petrobactin's synthesis is partially completed by both NRPS and NIS systems (85, 113).

1.6.4.2. Siderophore structure

Although there is incredible diversity in the structure of siderophores, they can be classified according to their iron-coordinating moieties. Three types of siderophore iron coordinating moieties have been documented (Fig. 1). The first type of functional group is a hydroxymate group, which uses both carbonyl and aminohydroxyl groups to coordinate iron as seen in desferrioxamine B (Fig. 2) (143). The second functional group incorporates a catecholate structure, which coordinates iron with two adjacent hydroxyl groups as seen in enterobactin (Fig. 2) (75). Lastly, there are polycarboxylate groups, which coordinate iron with either α-hydroxycarboxylates or carboxylic acid moieties as seen in staphyloferrin A (SA) (Fig. 2). This thesis will primarily focus on SA, an α-hydroxycarboxylate siderophore (100). Additionally, there are mixed-type siderophores that use combinations of the above functional groups to coordinate iron, such as aerobactin (Fig. 2) (65).

Although siderophores use a hexadentate structure to coordinate Fe(III) with an octahedral geometry, the stoichiometric relationship between siderophores and Fe(III) varies (65). Depending on the number of coordinating residues that a siderophore contains, they can form mono-, di-, or multi-nucleate iron complexes with one or more siderophore molecules involved (66). Additionally, some siderophores rely on solvent molecules to complete the hexa-coordinated complex (29).

catecholate
hydroxamate
carboxylate

Figure 1. Types of siderophore iron coordinating moieties. Illustrated are the three major siderophore functional groups involved in Fe(III) coordination; catecholate, hydroxamate, and carboxylate. Each group is bi-dentate. Red oxygen atoms can donate electrons to coordinate Fe(III).

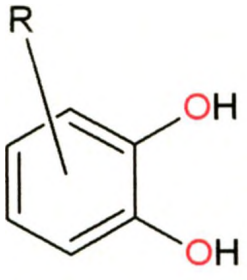

catecholate

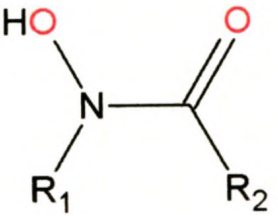

hydroxamate

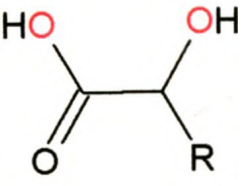

carboxylate

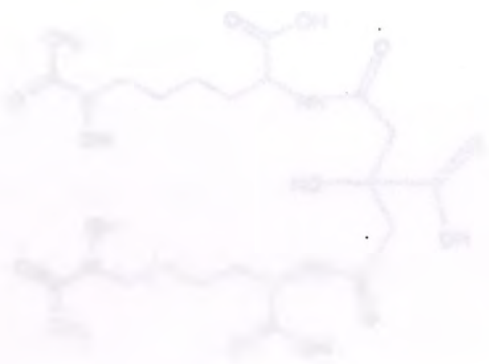

Figure 2. Types of siderophores. Illustrated are examples of the four types of siderophores classified according to their Fe(III)-coordinating moieties. Catecholate-enterobactin; hydroxamate-desferrioxamine B; polycarboxylate-staphyloferrin A; and mixed-type-aerobactin.

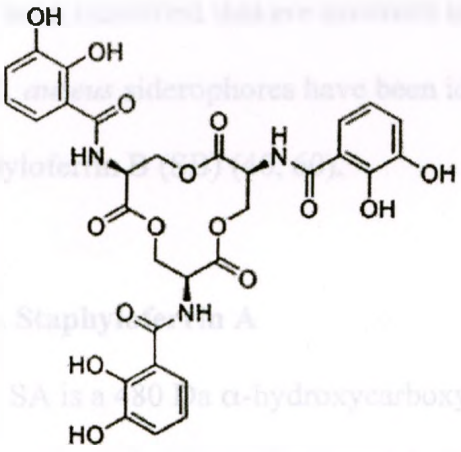

enterobactin

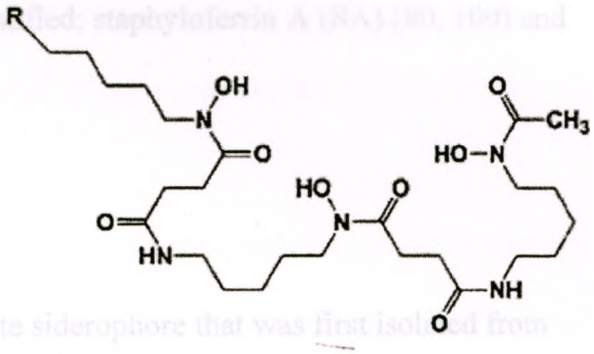

desferrioxamine B

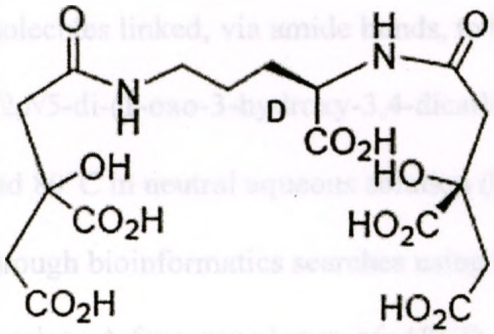

staphyloferrin A

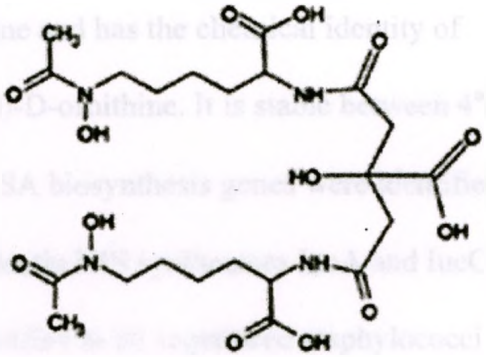

aerobactin

1.7. *S. aureus* siderophores

S. aureus has a profound ability to adapt to host environments and has multiple methods of accessing host iron. Not surprisingly, several staphylococcal genetic loci have been identified that are involved in siderophore biosynthesis or transport. To date, two *S. aureus* siderophores have been identified; staphyloferrin A (SA) (80, 100) and staphyloferrin B (SB) (40, 60).

1.7.1. Staphyloferrin A

SA is a 480 Da α-hydroxycarboxylate siderophore that was first isolated from iron-starved culture supernatant of *S. hyicus* (100). It is comprised of two citrate molecules linked, via amide bonds, to D-ornithine and has the chemical identity of *N*2,*N*5-di-(1-oxo-3-hydroxy-3,4-dicarboxybutyl)-D-ornithine. It is stable between 4°C and 80°C in neutral aqueous solution (80). The SA biosynthesis genes were identified through bioinformatics searches using the aerobactin NIS synthetases IucA and IucC as queries. A four-gene locus, *sfaABCD*, was identified in all sequenced staphylococci including *S. epidermidis*, *S. saprophyticus*, *S. aureus*, and *S. haemolyticus* (7). SA was also identified in culture supernatants of *S. aureus* and *S. epidermidis* and its production is stimulated by supplementation with D-ornithine (100). The *sfa* locus consists of a three-gene operon, *sfaABC*, and a divergently transcribed gene, *sfaD*. Upstream from two divergent promoters, intergenically between *sfaA* and *sfaD*, are two Fur box consensus sequences that provide Fur transcriptional control in *S. aureus* (7). However, constitutive production of SA in some CoNS suggests a lack of Fur regulation (96).

The genes of the *sfaABCD* locus encode two NIS synthetases, SfaB and SfaD, a putative pyridoxal-5'-phosphate (PLP)-dependant D-ornithine racemase, SfaC, and a putative SA efflux protein, SfaA (27). Cotton *et al.* demonstrated that purified SfaB and SfaD can generate SA *in vitro* from citrate and D-ornithine (27). The complete biochemical synthesis reaction is illustrated in Figure 3. SfaD is responsible for the committing step of synthesis, condensing citric acid and D-ornithine, and SfaB completes the molecule through condensation of citric acid and the δ-citryl-D-ornithine intermediate.

Chromosomal deletion of *sfaABCD* in *S. aureus* abrogates SA production however, if SB is still produced it does not result in an observable growth defect in mammalian serum (SB will be discussed below). Although this suggests that SA may not be the major contributor of transferrin iron, a more drastic growth deficit is observed in an SA and SB deficient mutant than a SB deficient mutant alone (7). Furthermore, SA has been demonstrated to remove iron from human and porcine transferrin (103, 6). Chromosomal deletion of *sfaABCD* in *S. aureus* can be complemented via plasmid-borne *sfa* genes from *S. aureus* or *S. epidermidis*, demonstrating functional conservation of the staphylococcal *sfa* locus despite protein sequence identities of 50-80% (7).

Figure 3. Staphyloferrin A biosynthesis pathway.

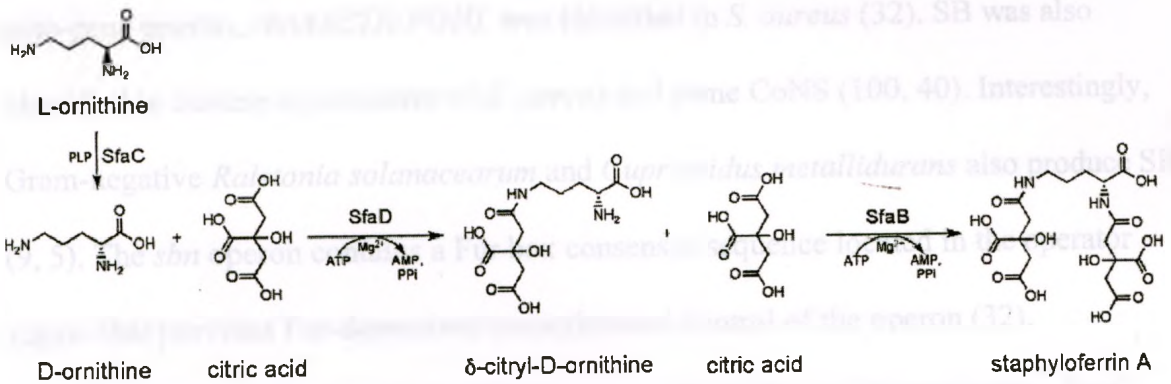
L-ornithine
PLP
SfaC
SfaD
ATP
Mg2+
AMP, PPi
SfaB
ATP
Mg2+
AMP, PPi
D-ornithine
citric acid
δ-citryl-D-ornithine
citric acid
staphyloferrin A

1.7.2. Staphyloferrin B

SB is a 448 Da α-hydroxycarboxylate siderophore that was initially purified and structurally characterized from iron-starved culture supernatant of *S. hyicus* (60). It is comprised of L-2,-3-diamino-propionic acid (DAPA), citrate, ethyldiamine (EDA), and α-ketoglutarate (α-KG) (40). The SB biosynthesis genes were also identified through bioinformatic searches of the aerobactin NIS synthetases IucA and IucC as queries. A nine-gene operon, *sbnABCDEFGHI*, was identified in *S. aureus* (32). SB was also identified in culture supernatants of *S. aureus* and some CoNS (100, 40). Interestingly, Gram-negative *Ralstonia solanacearum* and *Cupriavidus metallidurans* also produce SB (9, 5). The *sbn* operon contains a Fur box consensus sequence located in the operator region that provides Fur-dependent transcriptional control of the operon (32).

The genes of the *sbnABCDEFGHI* operon encode three NIS synthetases, SbnC, SbnE, and SbnF, a putative ornithine cyclodeaminase, SbnB, a putative L-O-acetylserine sulfhydrylase, SbnA, a putative SB efflux protein, SbnD (32), a PLP-dependant decarboxylase, SbnH, and two proteins with currently undefined functions, SbnG and SbnI (23). Cheung *et al.* demonstrated that purified SbnC, SbnE, SbnF, and SbnH can generate SB *in vitro* from DAPA, α-KG and citrate (23). SbnE is responsible for the first step of synthesis, condensing DAPA and citric acid to form a citryl-L-2,3-diamino-propionic acid intermediate. It is then decarboxylated by SbnH, forming citryl-diaminoethane, before a second DAPA molecule is condensed onto it by SbnF. Finally, SbnC completes SB through condensation of α-KG and L-2,3-diaminopropionyl-citryl-diaminoethane.

Chromosomal deletion of *sbnABCDEFGHI* in *S. aureus* abrogates SB production and impairs growth in serum. Although growth is not completely abolished, presumably due to the presence of SA, it suggests a significant role in iron acquisition from transferrin (7).

1.8. Siderophore-mediated iron acquisition

Gram-positive and Gram-negative bacteria require active transport systems to transport ferric-siderophores across their cell membrane because they are too large for passive diffusion. Although smaller siderophores (less than 600Da) may passively diffuse through porins in the Gram-negative outer membrane, siderophores generally require an energy-dependant carrier protein to cross this barrier (14). The cell wall of Gram-positive bacteria does not represent a barrier to movement of ferric-siderophores.

1.8.1. ATP-binding cassette transporters

Gram-positive and Gram-negative bacteria use ATP-binding cassette (ABC)-family transporters to import ferric siderophores across their cell membrane into the cytoplasm. They belong to one of the largest paralogous sequence superfamilies and consist of a receptor, a transmembrane permease, and a highly conserved ATPase (128). More than 600 ABC-transporters have been identified (33) and they are found ubiquitously among all genera of the three kingdoms of life (70).

There are three major classes of ABC-systems; importers, exporters, and a third class that is involved in mRNA translation and DNA repair. Each class is further subdivided into subclasses and families and this thesis will focus on class III binding-

protein-dependant (BPD) importers (33). These ABC-transporters have separate polypeptide TM, ABC, and substrate binding domains (117). The generic structure of ABC-transporters can be seen in Figure 4. Substrates for these ABC-transporters include mono- and oligosaccharides, ions, amino acids, short peptides, ferric-siderophores (the focus of this thesis), metals, polyamine cations, opines, and vitamins (39). The best-studied examples of these ABC-transporters are the high-affinity histidine and maltose transport systems of *Salmonella enterica* serovar Typhimurium and *E. coli* (54).

Many iron ABC-transporters are important virulence factors (64). Furthermore, many bacteria encode transporters for exogenous siderophores (i.e. xenosiderphores; siderophores produced by other organisms). For example, the *S. aureus* Fhu transporter is involved in the uptake of hydroxamate siderophores (produced mainly by fungi) despite lacking the necessary biosynthesis machinery to produce this type of molecule (134).

Figure 4. Schematic of Gram-negative and Gram-positive siderophore-mediated iron-uptake pathways. A) Gram-negative bacteria have outer-membrane receptors that bind and transfer siderophores to periplasmic binding proteins in a TonB-ExbB-ExbD-dependent process. The ligand-bound periplasmic binding protein then associates with its cognate ABC-transporter in the inner membrane, which transports the siderophore into the cytoplasm. B) Gram-positive bacteria have lipoprotein receptors, homologous to Gram-negative periplasmic binding proteins, which bind siderophores and associate with their cognate ABC-transporter in the cellular membrane, which transports the siderophore into the cytoplasm. PBP, periplasmic binding protein; TMD, transmembrane domain.

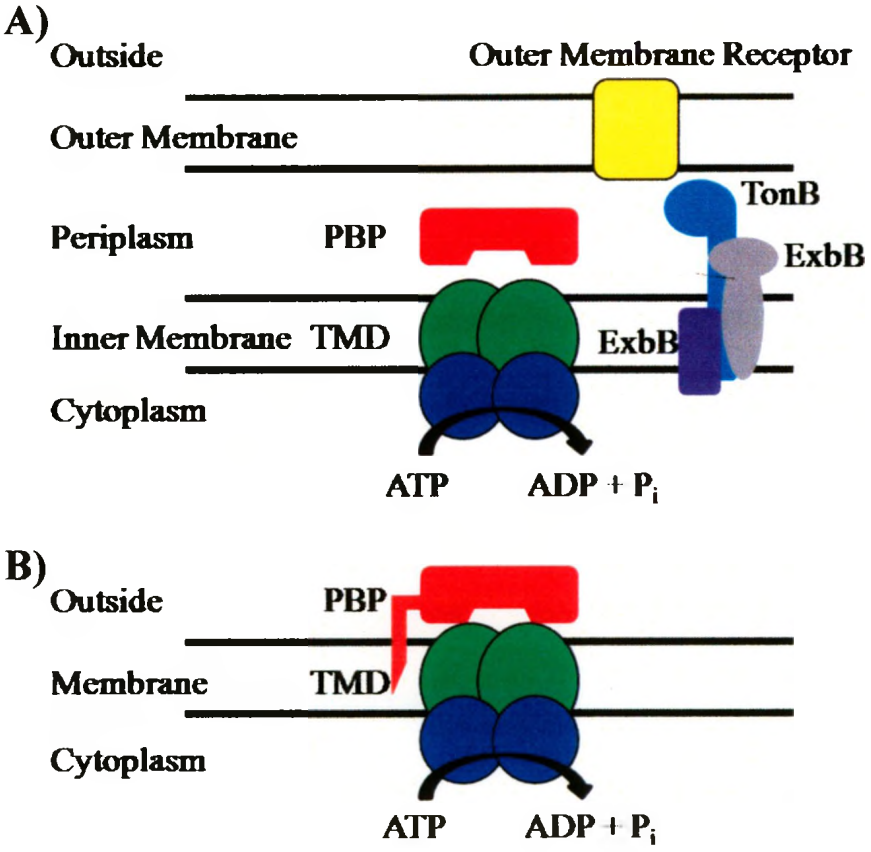
A)
Outside
Outer Membrane Receptor
Outer Membrane
TonB
Periplasm
PBP
ExbB
Inner Membrane
TMD
ExbB
Cytoplasm
ATP
ADP + P$_i$
B)
Outside
PBP
Membrane
TMD
Cytoplasm
ATP
ADP + P$_i$

1.8.2. *S. aureus* siderophore transporters

Given that *S. aureus* is such a successful human pathogen it is not surprising that many iron-regulated ABC-transporters are encoded within its genome. To date, one heme transporter (IsdEF) (32) and four siderophore transporters have been identified and characterized (57, 58, 6). The latter transporters are HtsABC (Fe(III)-SA), SirABC (Fe(III)-SB), FhuCBG-D1-D2 (Fe(III)-hydroxamate siderophores) and SstABCD (Fe(III)-catecholamines/catechols) (6).

1.8.3. The staphyloferrin B receptor: SirA

The *sir* locus encodes a lipoprotein receptor, SirA, and two heterodimeric permeases, SirBC (32). FhuC provides the ATPase activity that is necessary for Fe-SB transport (138). A chromosomal deletion of *sirA* or *sirB* abolishes SB transport in *S. aureus* (32). Also, heterologous expression of *sirABC* in *S. epidermidis* allows SB-dependant growth (5). The crystal structures of apo- and holo-SirA have been solved, positively identifying SB in the substrate binding-pocket (57).

The Fe-SB-rSirA crystal structure was among the first Gram-positive siderophore receptors to be structurally characterized (57). It has a class-III binding fold between separate N- and C-terminal domains that are linked by a single α-helix (57). Both N- and C-terminal domains contain a central parallel β-sheet that is surrounded by short α-helices (57). Although most class III binding protein crystal structures reveal that ligand binding results in either subtle or hinged-motion conformational changes, both the Fe-SB-SirA and Fe-SA-HtsA crystal structures reveal localized conformational

changes in the C-terminal loops of the binding site. However, different regions of each receptor's C-terminal domain undergo the largest conformational changes (57, 58). Furthermore, fluorescence quenching experiments using Fe-SB, Fe-SA, and Fe-desferrioxamine demonstrated that SirA is highly specific for Fe-SB. Therefore, the unique structural features of HtsA and SirA are likely responsible for their ability to distinguish between the two α-hydroxycarboxylate siderophores (57, 58).

SirA forms a total of nine contact points with Fe-SB. Three arginine residues form five hydrogen-bonds (H-bonds) with three Fe-SB oxygen atoms and two nitrogen atoms. R125 forms two salt bridges with the Fe(III) coordinating carbonyl of the α-KG component and citrate group (57). R201 forms a H-bond with the carbonyl oxygen that links the Fe-SB DAPA and citrate groups and R206 forms salt bridges to the α-KG and citrate components. Finally, T144 forms an H-bond with the C11-C12 amide linkage, Y208 forms an H-bond with the citrate carboxylate group, and N304 forms an additional polar contact with the citrate carboxylate group. Comparison of apo- and holo-SirA revealed that the majority of intradomain conformational change was maximal in the C-terminal loops. The movements help to occlude Fe-SB in the binding pocket, reducing solvent exposure to 23.6%. Among the SirA residues, N263 moves the greatest distance of 11.3Å and others are brought into closer proximity with Fe-SB, likely facilitating some of the H-bonds identified (57).

1.8.4. The staphyloferrin A receptor: HtsA

The *hts* locus was first described and named as a "heme-transport system", following the observation that transposon disruption of *hts* resulted in preferential uptake of transferrin Fe(III) over heme Fe(II) (137). However, a chromosomal deletion of *htsABC* abolishes SA transport in *S. aureus* (7). Furthermore, the crystal structures of apo- and two forms of holo-HtsA have been solved, positively identifying SA in the substrate binding-pocket (Figure 5A, B, and C)(7, 58). It was the first Gram-positive (7) and first α-hydroxycarboxylate siderophore receptor to be structurally characterized (58). Table 1 lists the dissociation constants (K_d) of Fe-SA-rHtsA and several related proteins. Their significance will be discussed in more detail in later sections.

Figure 5. HtsA crystal structure. A) Surface electrostatics of HtsA. The binding groove is a large positively charged region. Blue, white, and red indicate positive, neutral, and negative potential, respectively. B) HtsA undergoes localized conformational changes following binding of Fe-staphyloferrin. Illustrated is an overlay of the open and closed forms and the apo-conformations of the HtsA crystal structures. Open conformation, red; closed conformation, blue; apo-conformation, green. Staphyloferrin A is shown in the binding pocket of the open-conformation. C) Coordination and binding of staphyloferrin A in the HtsA binding pocket. On the left is the open conformation of staphyloferrin A in the HtsA binding pocket. On the right is the closed conformation of staphyloferrin A in the HtsA binding pocket. HtsA residues forming contacts with SA are cyan *sticks*, with carbon, nitrogen, oxygen, and iron shown as green, blue, red, and orange, respectively. Hydrogen-bonds are represented by dashed lines (58). In the open conformation R299 is modeled in two positions within H-bonding distance from Fe-SA.

A)

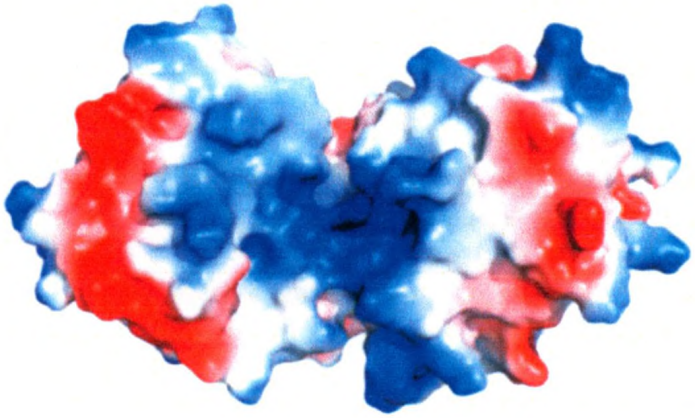

B)

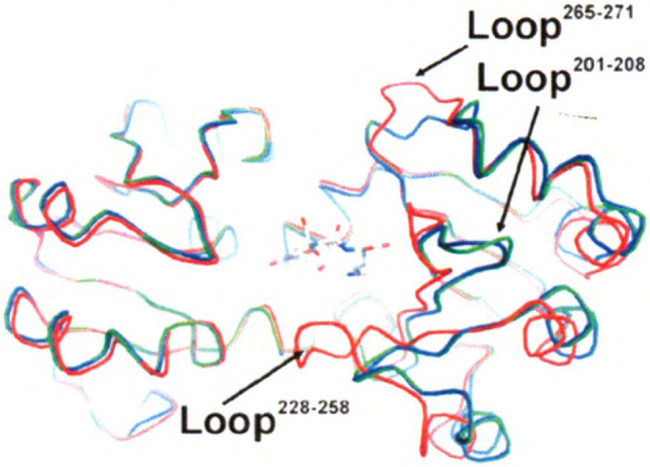
Loop265-271
Loop201-208
Loop228-258

C)

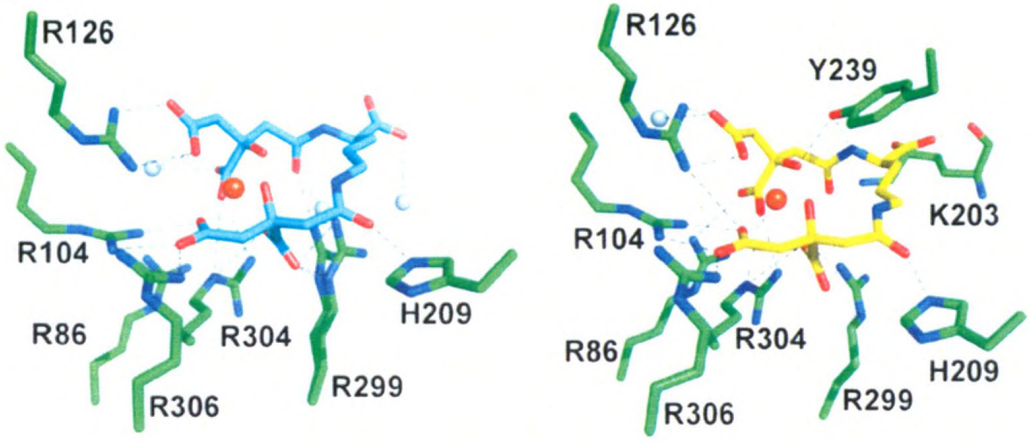
R126
R104
R86
R304
R306
R299
H209
R126
Y239
K203
R104
R86
R304
R306
R299
H209

Table 1. Dissociation constants for receptor-ferric-siderophore complexes

Protein[a]	Organism	Ligand	Dissociation Constant (K_d)	Reference
HtsA	*S. aureus*	staphyloferrin A	Low nM	(58)
FeuA	*B. cereus*	bacillibactin	19 nM	(155)
FeuA	*B. cereus*	enterobactin	12 nM	(155)
FatB	*B. cereus*	3,4-DHB	1.3 nM	(155)
FatB	*B. cereus*	petrobactin	127 nM	(155)
FpuA	*B. cereus*	petrobactin	175 nM	(155)
YfiY	*B. cereus*	schizokinen	34 nM	(155)
YxeB	*B. cereus*	desferroximine	18 nM	(155)
YclQ	*B. subtilis*	petrobactin	113 nM	(156)
FhuD	*E. coli*	Ferric-hydroxamates	300-7900 nM	(122)
FpvA[b]	*P. aeruginosa*	pyoverdin	0.37 nM	(68)
FhuA[b]	*P. aeruginosa*	ferrichrome	0.65 nM	(68)
FptA[b]	*P. aeruginosa*	pyochelin	0.54 nM	(68)

[a] Proteins are class III ligand-binding proteins unless otherwise stated.
[b] Gram-negative Outer membrane receptor proteins.

HtsA has a class-III binding fold between separate N- and C-terminal domains that are linked by a single α-helix (58). Similar to SirA, both N- and C-terminal domains contain a central parallel β-sheet that is surrounded by short α-helices (57, 58). Its structure is similar to other class III binding proteins including BtuF (*E. coli* B_{12} uptake) (10, 78), TroA (*E. coli* Zn^{2+} uptake) (86, 87), FhuD (*E. coli* ferrichrome uptake) (24, 82), and ShuT (*Shingella dysenteriae* heme uptake) (67) however, it has a novel form of ligand entrapment (58). The two holo-HtsA forms represent distinct open and closed conformations. The conformational change results from isolated movements of three loops within the C-terminal domain and is unique among class III binding proteins (Fig. 5B) (58).

HtsA forms six contact points with Fe-SA in the open conformation (Fig 5C). Five arginine residues form hydrogen bonds (H-bonds) with oxygen atoms of Fe-SA. R104 and R126 form H-bonds with Fe-SA. R299 is modeled in two positions within H-bond proximity of a Fe-SA ornithine hydroxyl group and R304 and R306 form H-bonds with a terminal Fe-SA carboxylate group. H209 forms another H-bond with the Fe-SA ornithine hydroxyl group and four water molecules are modeled within H-bond proximity of the Fe-SA ornithine carboxylate group, carbonyl group, and two carboxylate groups of one of the citrate molecules (58). Loop movements leading to the closed conformation result in the additional contacts with Fe-SA, shift it deeper into the binding pocket, and reduce solvent exposure from 33.0 to 14.5%. Y239 moves the greatest distance, 12.1Å, before forming a H-bond with a citrate carbonyl group. The closed conformation also allows K203 and R86 to H-bond with Fe-SA carboxylate

groups (Fig. 5C). Although several of the contact points remain the same, several of the H-bond lengths are reduced in the closed structure (58).

1.9 Research objectives

The goal of this research is to further characterize *S. aureus* SA transport and to provide a model system for α-hydroxycarboxylate siderophore transport. The first research objective was to synthesize and purify SA for use in receptor binding and bacterial growth assays. The second research objective was to use site-directed mutagenesis to mutate HtsA residues predicted by the holo-HtsA crystal structure to mediate binding and/or transport of Fe-SA. Finally, the last research objective was to determine the effects of each residue substitution on Fe-SA binding affinity and their biological significance under iron-restricted or SA-dependent growth conditions.

Chapter 2 – Materials and Methods

2.1. Bacterial strains and growth conditions

The bacterial strains used in this study are described in Table 2. Unless otherwise indicated, bacteria were cultured at 37°C. Antibiotics were used at the following concentrations: for *E. coli*, ampicillin (Ap) 100 μg mL^{-1}, kanamycin (Km) 30 μg mL^{-1}, choramphenicol (Cm) 30 μg mL^{-1}, and for *S. aureus*, Km 50 μg mL^{-1}, Cm 5 μg mL^{-1}, neomycin (Nm) 50 μg mL^{-1}, tetracycline (Tc) 4 μg mL^{-1}, erythromycin (Em) 3 μg mL^{-1}. For molecular-genetic manipulations, *E. coli* was grown in Luria-Bertani broth (LB), and *S. aureus* was grown in tryptic soy broth (TSB). For experiments completed under iron-limiting growth conditions, Tris-minimal succinate (TMS), prepared as described (135), was used. To further control the bioavailable iron, growth media was supplemented with 50 μM $FeCl_3$, 10 μM ethylenediamine-di-*o*-hydroxyphenylacetic acid (EDDHA) (LGC Promochem), or treated with 10% w/v Chelex® 100 resin (Bio-Rad) overnight at 4°C and supplemented with 20% v/v heat-inactivated horse-serum. All solutions and growth media were made with water purified by a Milli-Q purification system (Millipore Corp). Solid media was obtained by addition of 1.5% w/v Bacto-agar (Difco). Cultures were stored at -80°C in 15% v/v glycerol.

Table 2. Bacterial strains used in this study

Strain	Description[a]	Source or reference
S. aureus		
Newman	Wild-type clinical isolate	(42)
RN4220	$r_k^- m_k^+$; accepts foreign DNA	(81)
H1497	Newman *ΔhtABC*::Tc *ΔsirA*::Km; Tc^R Km^R	(7)
E. coli		
DH5α	φ_{80} d*LacZΔM15 recA1 endA1 gyrA96 thi-1 hsdR17*($r_k^- m_k^+$) *supE44 relA1 deoR* Δ(*lacZYA-argF*) *U169*	Promega
ER2566	$F^-\lambda^-$ *fhuA2 [Ion] ompT* lacZ::T7 geneI *gal sulA11* Δ*(mcrC-mrr)*114::IS *10* R*(mcr-73*::miniTn*10)*2 R*(zgb*-210::Tn *10)*1 (Tet^S) *endA1* [*dcm*]	New England Biolabs
BL21	F^-, *omp*T, *hsd*S_B (r_B^-, m_B^-), *dcm*, *gal*, λ(DE3), pLysS, Cm^R.	Promega

[a] Abbreviations: Tc^R, Km^R, and Cm^R, resistance to tetracycline, kanamycin, and chloramphenicol, respectively.

2.2. Recombinant DNA methodology

2.2.1. Plasmid isolation from *E. coli*

The plasmids used in this study are described in Table 3. Manipulation of recombinant DNA was completed as described (127). Plasmid DNA was isolated from *E. coli* using QIAprep mini-spin kits (QIAgen) or E.Z.N.A™ Plasmid Miniprep Kit II (Omega Bio-Tek), according to the manufacturer's directions. All centrifugation was completed at 14 000 × *g*, unless otherwise indicated. Typically, approximately 2 mL of stationary phase *E. coli* was harvested by centrifugation (10 000 × *g*) and resuspended in 250 µL of P1 buffer. Cell lysis was achieved via addition of 250 µL of buffer P2 (Qiagen), gentle inversion, and incubation for 5 minutes. The solution was neutralized via addition of 350 µL of N3 buffer, mixed by inversion, and centrifuged for 10 minutes to pellet insoluble material. The supernatant was applied to the QIAprep spin column and centrifuged for 1 minute. The spin column was washed with 750 µL of PE buffer and centrifuged twice for 1 minute to remove excess ethanol. Plasmid DNA was eluted from the resin and into a microcentrifuge tube via centrifugation (12000 × g) after addition of 50 µL of 42°C ddH_2O to the resin.

Table 3. Plasmids used in this study

Plasmid	Description[a]	Source or reference
pET28a(+)	Vector for overexpression of His-tagged proteins using the T7 bacteriophage promoter	Novagen
pEV99	pET28a(+) derivative encoding the soluble portion of HtsA; Km^R	(7, 58)
pLI50	*E. coli*/*S. aureus* shuttle vector; Ap^R Cm^R	(84)
pEV55	pLI50 derivative containing *htsABC* from *S. aureus*; Cm^R	(7)
pAUL-A	Temperature-sensitive S. aureus suicide vector; Em^R Lc^R	(17)
pUC19	*E. coli* cloning vector; Ap^R	(153)
pJDC41	pET28a(+) derivative encoding SfaB; Km^R	(58)
pJDC42	pET28a(+) derivative encoding SfaD; Km^R	(58)
pDG1513	pMTL22 derivative that carries a Tc resistance cassette; Ap^R	(59)

[a] Abbreviations: Km^R, Ap^R, Cm^R, Em^R, and Lc^R, resistance to kanamycin, ampicillin, chloramphenicol, erythromycin, and lincomycin, respectively.

2.2.2. Plasmid isolation from *S. aureus*

Plasmid DNA was isolated from *S. aureus* as described for *E. coli*, but with the following modifications. Approximately 1 mL of stationary phase *S. aureus* culture was harvested by centrifugation (10 000 × *g*) and resuspended in 250 µL of P1 buffer that was modified by the addition of 50 µg mL^{-1} lysostaphin (Sigma). Cells were then incubated at 37°C for 30 minutes prior to addition of P2 buffer.

2.2.3. Restriction enzyme digests

Restriction endonucleases were purchased from Roche Diagnostics or New England Biolabs (NEB) and reactions were completed according to the manufacturer's instructions. Typically, reactions were completed in 20 µL and incubated for 1 hour at 37°C. The resulting DNA fragments were then cleaned using the QIAquick PCR purification kit (QIAgen) according to the manufacturer's instructions.

2.2.4. DNA ligations

T4 DNA ligase was purchased from Roche Diagnostics or NEB and reactions were completed according to the manufacturer's instructions. Typically, reactions were completed in 20 µL, with a 3:1 insert to vector DNA ratio, and incubated overnight at 4°C.

2.2.5. Agarose gel electrophoresis

Agarose gel electrophoresis was used to separate, visualize, and quantify DNA fragments. Agarose gels consisted of 0.8% w/v agarose in TAE buffer (40 mM Tris-acetate, 1 mM EDTA), supplemented with 1 µL SYBR Safe DNA gel stain (Invitrogen). Prior to loading, DNA samples were mixed with loading buffer (5% v/v glycerol, 0.04% w/v bromophenol blue, 0.04% w/v xylene cyanol, 10 mM EDTA, pH 7.5) in a 5:1 DNA to buffer ratio, and 12 µL was loaded per well. The gels were run at 110 V for 20 minutes and a 1 kb-Plus ladder (Invitrogen) was used as a standard reference for estimating DNA size. After electrophoresis, gels were placed on a ChemiDoc XRS unit and DNA was visualized using Quantity One software (Bio-Rad).

2.2.6. In-well cell-lysis plasmid screening

In-well cell-lysis was used to rapidly screen *E. coli* for the presence of recombinant plasmid DNA. In summary, a 0.8% w/v TBE-agarose gel was supplemented with 0.4% w/v SDS prior to solidification and immersion in TBE buffer. A toothpick was then used to harvest a small quantity of *E. coli* cells from an agar plate that were resuspended in 10 µL of sterile water and 10 µL of SRL buffer (1 mg mL^{-1} lysozyme, 25% w/v sucrose in TBE, and 10 µgmL^{-1} RNase A). Ten microlitres of each suspension was then loaded per well and allowed to incubated for 10 minutes at room temperature or until lysis was complete. The gels were then run at 20 V for 20 minutes, followed by 105 V for 30 minutes. The gels were then stained with ethidium bromide

(EtBr) and placed on a ChemiDoc XRS unit and DNA was visualized using Quantity One software (Bio-Rad).

2.2.7. Isolation of DNA fragments from agarose gels

Following electrophoresis, desired DNA fragments were visualized and identified under UV light (365 nm) and excised from agarose gels using a glass cover slip. The DNA fragments were then isolated using the QIAquick Gel Extraction Kit (Qiagen), according to manufacturer's instructions.

2.2.8. Isolation of chromosomal DNA from *S. aureus*

S. aureus Newman chromosomal DNA was obtained using the InstaGene Matrix (Bio-Rad) as described by the manufacturer. Typically, 1 µL of the resulting chromosome supernatant was used as template DNA in polymerase-chain reactions (PCR).

2.2.9. Polymerase-chain reaction

PCRs were completed in 50 µL reactions containing template DNA, 1× PCR buffer (Roche Diagnostics), 200 µM dNTP (Roche Diagnostics), 12 picomoles of forward and reverse primers (IDT DNA), and 2.5 units of *Pwo*I DNA polymerase (Roche diagnostics). PCRs were performed using the GeneAmp PCR system (Perkin-Elmer), the PTC-200 Peltier Thermal Cycler (MJ Research Inc.), or the MJ Mini™ Personal Thermal Cycler (Bio-Rad). Oligonucleotide primers are listed in Table 4.

Table 4. Oligonucleotides used in this study

Purpose	Sequence[a]
Cloning of *htsA* (Soluble Portion)	5'-AAGCTAGCACTATTTCGGTAAAAGATGAAAATG-3' (forward, *Nhe*I)
Cloning of *htsA* (Soluble Portion)	5'-AAGGATCCCATTTACTTCCACCTTACTTTTGTTC-3' (reverse, *Bam*HI)
Cloning of *htsABC* (from *S. aureus*)	5'-TGAGCTCTGCGATTACATTGGAGGCTG-3' (forward, *Sac*I)
Cloning of *htsABC* (from *S. aureus*)	5'-TGCCCGGGGTTAGTTATTTCATTCTTCG-3' (reverse, *Sma*I)
Cloning of *sfaB* (from *S. aureus*)	5'-TAAGCTAGCATGGTATATCTTGAATGGGC-3' (forward, *Nhe*I)
Cloning of *sfaB* (from *S. aureus*)	5'-TATGGATCCCTACACCTCTTTTTTTATCG-3' (reverse, *Bam*HI)
Cloning of *sfaD* (from *S. aureus*)	5'-GCCGCTAGCATGAACTTGAAC-3' (forward, *Nhe*I)
Cloning of *sfaD* (from *S. aureus*)	5'-TCTGGATCCTTAATTATTTTCTCGATACAAAG-3' (reverse, *Bam*HI)

[a] Restriction sites for cloning of PCR products are underlined.

2.2.10. Site-directed mutagenesis

Site-directed mutagenesis was carried out using the QuickChange® site-directed mutagenesis kit (Stratagene), using Pfu Turbo® DNA polymerase, or Phusion® DNA polymerase (New England Biolabs). Following amplification, DNA was treated with *Dpn*I endonuclease (New England Biolabs) to degrade template DNA. Remaining DNA was vacuum-centrifuged to a volume of approximately 20 µL prior to transformation of *E. coli* DH5α $CaCl_2$ competent cells and plating on selective media. Primers were ordered from IDT DNA and are listed in Table 5.

Table 5. Oligonucleotides used for site-directed mutagenesis

Purpose	Sequence[a]
Mutation of HtsA, R104A	5'-GATTATACTTCTGTAGGTACAGCTAAACAGCC-3' (forward)
Mutation of HtsA, R104A	5'-CTTCTAAGTTTGGCTGTTTAGCTGTACCT-3' (reverse)
Mutation of HtsA, E110A	5'-CCAAACTTAGCAGAAATTAGTAAATTAAAAC-3' (forward)
Mutation of HtsA, E110A	5'-CCGGTTTTAATTTACTAATTTCTGCTAAGTTTG-3' (reverse)
Mutation of HtsA, R126A	5'-GATTTAATTATCGCTGATAGCAGTGCACAT-3' (forward)
Mutation of HtsA, R126A	5'-TATTAATACCTTTATGTGCACTGCTATCAGC-3' (reverse)
Mutation of HtsA, K203A	5'-CTTCCAGCAGTAGTTGCTGCAGCTG-3' (forward)
Mutation of HtsA, K203A	5'-GATGTGCTAATAAACCAGCTGCAGCA-3' (reverse)
Mutation of HtsA, H209A	5'-GCTAAAGCTGGTTTATTAGCAGCTCCA-3' (forward)
Mutation of HtsA, H209A	5'-GTCCAACATATGAATAGTTTGGAGCTGCT-3' (reverse)
Mutation of HtsA, Y239A	5'-CGATGTAACAAAAGGTTTAAGTAAAGCTTTGA-3' (forward)
Mutation of HtsA, Y239A	5'-AGTAAGGTCCTTTCAAAGCTTTACTTAAACC-3' (reverse)
Mutation of HtsA, E250A	5'-CTTACTTACAATTAGACACTGCACATTTAGC-3' (forward)
Mutation of HtsA, E250A	5'-CAGCTAAATGTGCAGTGTCTAATTGTAAG-3' (reverse)
Mutation of HtsA, R86K	5'-GTCGATGATGGTAAGAAAAAAAAAATC-3' (forward)
Mutation of HtsA, R86K	5'-CTCTAACTGGTTTAATGATTTTTTTTTTC-3' (reverse)
Mutation of HtsA, R104K	5'-GATTATACTTCTGTAGGTACAAAAAAACAGCC-3' (forward)
Mutation of HtsA, R104K	5'-CTTCTAAGTTTGGCTGTTTTTTTGTACCT-3' (reverse)
Mutation of HtsA, R126K	5'-TCGCTGATAGCAGTAAACATAAAGGTA-3' (forward)
Mutation of HtsA, R126K	5'CTTTATTAATACCTTTATGTTTACTGCTATCAGC-3' (reverse)
Mutation of HtsA, K203R	5'-CCAGCAGTAGTTGCTAGAGCTGGTT-3' (forward)
Mutation of HtsA, K203R	5'-GATGTGCTAATAAACCAGCTCTAGCAACTA-3' (reverse)
Mutation of HtsA, H209Q	5'-GCTAAAGCTGGTTTATTAGCACAACCA-3' (forward)
Mutation of HtsA, H209Q	5'-GTCCAACATATGAATAGTTTGGTTGTGCT-3' (reverse)
Mutation of HtsA, Y239F	5'CGATGTAACAAAAGGTTTAAGTAAATTTTTGA-3' (forward)
Mutation of HtsA, Y239F	5'-AGTAAGGTCCTTTCAAAAATTTACTTAAACC-3' (reverse)

[a] Mutated bases are underlined.

2.2.11. DNA sequencing

DNA sequencing was provided by the DNA Sequencing Facility of the Robarts Research Institute (London, Ontario) or the York Sequencing Facility (Toronto, Ontario).

2.2.12. Computer analysis

DNA sequence analysis, oligonucleotide primer design, and protein analysis were completed using Vector NTI Suite software package (Informax, Bethesda, MD). Data was analyzed using Microsoft Office Excel and graphs were generated using GraphPad Prism 4.0.

2.3. Transformation methodologies

2.3.1. Preparation of transformation competent *E. coli*

E. coli DH5α $CaCl_2$ competent cells were prepared as follows: An overnight, stationary phase DH5α culture was normalized to an OD_{600} of 1, diluted 1:100 into 500 mL of fresh LB, and grown to an OD_{600} of approximately 0.5. The culture was then placed on ice for 30 min and cells were harvested by centrifugation at 5 000 × *g*. The cells were then resuspended in 100 mL of $CaCl_2$ solution (100 mM $CaCl_2$, 15% glycerol) and incubated on ice for 30 min. Cells were harvested again by centrifugation, resuspended in 4 mL of $CaCl_2$ solution, and aliquots of 100 µL were stored at -80°C.

2.3.2. Transformation of $CaCl_2$ competent *E. coli*

Purified plasmid DNA or ligation reactions were added to an aliquot of *E. coli* DH5α $CaCl_2$ competent cells and kept on ice for 30 min. Cells were then subjected to heat shock treatment at 42°C for 2 min followed immediately by 2 min incubation on ice. The cells were resuspended in 900 µL of fresh LB, mixed by inversion, and incubated for 1 h at 37°C prior to plating on selective media and incubation overnight.

2.3.3. Preparation of transformation competent *S. aureus*

Strains of *S. aureus* were made electro-competent as follows: An overnight, stationary phase culture of *S. aureus* was normalized to an OD_{600} of 1, diluted 1:100 into 400 mL of fresh TSB, and grown to an OD_{600} of approximately 0.4. The cells were then harvested by centrifugation at 5 000 × *g* and resuspended in an equal volume of 500 mM sucrose and incubated on ice for 30 min. The cells were then harvested by centrifugation and resuspended in 4 mL of 500 mM sucrose. The last step was reeated and aliquots of 60 µL were stored at -80°C.

2.3.4. Transformation of electro-competent *S. aureus*

Purified plasmid DNA was added to an aliquot of electro-competent *S. aureus* cells and kept on ice for 30 min. Cells were then transferred to an ice-cold electroporation cuvette (2 mm, Bio-Rad) for electroporation. Electroporation was performed using a Bio-Rad Gene Pulser II with the following settings: 2.5 V, 200 mA, and 25 Ω. Pulsed cells were then resuspended in 900 µL of fresh TSB, transferred to a

sterile micro-centrifuge tube, and incubated for 1 h at 37°C prior to plating on selective media and incubation overnight.

2.4. Mutagenesis and DNA cloning methodologies

2.4.1. Mutagenesis of *htsABC*

The construction of a *S. aureus* Newman strain bearing an *htsABC*::Tc operon deletion has been previously described (7). For complementation, the *htsABC* locus and flanking promoter region was PCR amplified from *S. aureus* Newman chromosomal DNA and the 4.0-kb fragment was cloned into pLI50, generating pEV55 as illustrated in Figure 6. Oligonucleotide primers used are listed in Table 4.

2.5. Siderophore synthesis, purification, quantification

2.5.1. Staphyloferrin A synthesis

Using rSfaB and rSfaD, *in vitro* SA biosynthesis was carried out as previously described (27), with minor modifications. Briefly, reactions were completed in 500 µL containing 1 mM sodium-citrate, 1 mM D-ornithine, 5 mM ATP, 0.5 mM $MgCl_2$, 50 mM HEPES, 5 µM rSfaB, and rSfaD at pH 7.4, and incubated for 12 hours in the dark at room temperature.

Figure 6. Physical maps of plasmids pEV99 and pEV55. For pEV99, a fragment containing the soluble potion of the *htsA* coding region was cloned into the pET28a(+) protein overexpression vector between the *Bam*HI and *Nhe*I restriction sites. The plasmid also contains a pBR233 origin of replication that allows for replication in Gram-negative bacteria, a *lacI* region that encodes for a Lac repressor protein. For pEV55, a fragment containing the upstream regulatory sequence and the *htsABC* operon was cloned into the *E. coli*/*S. aureus* shuttle vector, pLI50, between the *SacI* and *SmaI* restriction sites. The plasmid also contains an Ap^R marker (*bla*) for selection in *E. coli* and a Cm^R marker (*cat*) for selection in *S. aureus*. The plasmid also contains two origins of replication, pBR233 and RepB, which allow for replication in Gram-negative and Gram-positive bacteria, respectively.

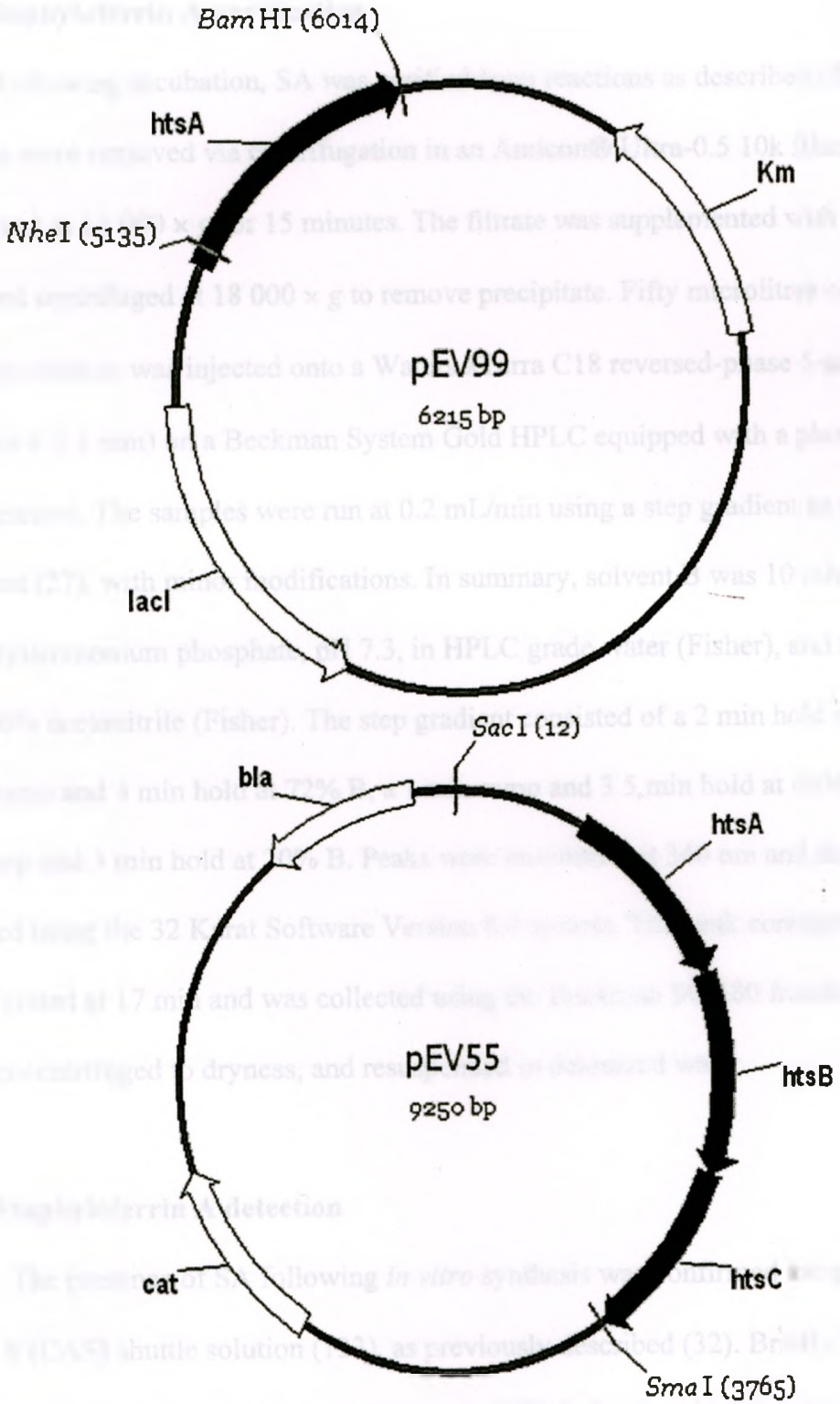
BamHI (6014)
htsA
Km
NheI (5135)
pEV99
6215 bp
lacI
SacI (12)
bla
htsA
pEV55
9250 bp
htsB
cat
htsC
SmaI (3765)

2.5.2. Staphyloferrin A purification

Following incubation, SA was purified from reactions as described (58). Briefly, enzymes were removed via centrifugation in an Amicon® Ultra-0.5 10k filter column (Millipore) at 14 000 × *g* for 15 minutes. The filtrate was supplemented with 3 mM $FeCl_3$ and centrifuged at 18 000 × *g* to remove precipitate. Fifty microlitres of the resulting solution was injected onto a Waters xTerra C18 reversed-phase 5-μm column (150 mm × 2.1 mm) on a Beckman System Gold HPLC equipped with a photodiode array detector. The samples were run at 0.2 mL/min using a step gradient as previously described (27), with minor modifications. In summary, solvent B was 10 mM tetrabutylammonium phosphate, pH 7.3, in HPLC grade water (Fisher), and solvent A was 100% acetonitrile (Fisher). The step gradient consisted of a 2 min hold at 85% B, a 1 min ramp and 4 min hold at 72% B, a 1 min ramp and 3.5 min hold at 66% B, and a 1 min ramp and 3 min hold at 20% B. Peaks were monitored at 340 nm and data were analyzed using the 32 Karat Software Version 8.0 system. The peak corresponding to Fe-SA eluted at 17 min and was collected using the Beckman SC 100 fraction collector, vacuum-centrifuged to dryness, and resuspended in deionized water.

2.5.3. Staphyloferrin A detection

The presence of SA following *in vitro* synthesis was confirmed using chrome azurol S (CAS) shuttle solution (133), as previously described (32). Briefly, dilutions of SA reactions were mixed with equal volumes of CAS shuttle solution and incubated for 45 min in the dark at room temperature. SA presence was verified through determination

of siderophore units by the following formula: [(A630 of control reaction (missing ATP) – A630 of sample)/(A630 of control reaction)(inverse of dilution factor)] × 100%.

The presence of Fe-SA following ion-pair HPLC purification was confirmed using liquid chromatography/mass spectrometry (LC/MS) as previously described (27), with minor modifications. In summary, EDTA was added to Fe-SA samples to increase SA detection sensitivity in the LC-MS (97).

2.5.4. Staphyloferrin A quantification (AAS)

Atomic absorption spectroscopy was used to indirectly determine the concentration of Fe-SA by measuring the concentration of iron in the HPLC-purified Fe-SA samples as previously described (58). Briefly, Fe-SA samples were diluted in 1 M nitric acid and then drawn by an SPS 5 sample preparation system (autosampler) into a Varian AA240 atomic absorption spectrometer. An iron/manganese hollow cathode lamp was used to detect iron absorbance by emitting at 248.3 nm. Calibration standards were analyzed to generate a linear calibration curve. The curve was generated using known iron standards, diluted in 1 M nitric acid, from an atomic absorption spectrometer certified 1000 ppm ± 1% stock (Fisher) before the Fe-SA samples were analyzed.

2.6. *S. aureus* growth curves

Bacteria were cultured for 12 h in TMS broth followed by an additional 12 h in fresh TMS broth. Cells were washed three times with 0.9% w/v saline and diluted 1:100 into 80% horse serum (Sigma-Aldrich) and 20% Chelex® 100 resin (Bio-Rad) treated TMS broth. For iron replete media, 50 μM $FeCl_3$ was added. Cultures were grown with

constant, medium amplitude shaking in a Bioscreen C machine (Growth Curves, USA) and OD was measured at 600 nm every 30 min.

2.7. Disk-diffusion growth assays

The ability of Fe-SA to promote the iron-restricted growth of *S. aureus* Newman Δ*sirA*Δ*htsABC* harbouring plasmid-borne WT or mutant *htsABC* was determined using disk-diffusion assays as previously described (7), with minor modifications. In summary, *S. aureus* cells were inoculated into TMS agar containing 10 μM EDDHA to achieve 1 × 10^4 cells mL^{-1}. Desferrioxamine (50 μM) was used as a positive control for growth. Ten microlitres of SA or Desferrioxamine were added to sterile paper disks which were then placed onto the plates. Growth diameter was measured after 24 h at 37°C.

2.8. Protein methodologies

2.8.1. Protein purification

The SA synthetases, SfaB and SfaD, and the SA-receptor, HtsA, were purified for use in SA synthesis reactions and Fe-SA fluorescence titration experiments, respectively. A rHtsA overexpression vector constructed as described (7, 58) was used to express and purify rHtsA from *E. coli* ER2566 as previously described (7). Briefly, DNA encoding a portion of mature HtsA (residues 38-327), was PCR amplified from *S. aureus* Newman chromosomal DNA and the 1-kb fragment was cloned into pET28a(+), generating pEV99 as illustrated in Figure 6. The *sfaB* and *sfaD* coding regions were amplified from *S. aureus* Newman chromosomal DNA and cloned into pET28a(+) for over-expression in *E. coli* BL21(DE3) as previously described (58). In summary,

cultures were grown in LB (Difco) supplemented with 30 μg/mL Km at 37°C. At an OD_{600} of ~0.9 isopropyl 1-thio-β-D-galactopyranoside (IPTG) (500 μM) was added and the culture was incubated for an additional 18 h at room temperature with shaking (180 rpm).

Cells were harvested by centrifugation at 15 000 × *g*, resuspended in binding buffer (50 mM HEPES, 500 mM NaCl, 10 mM imidazole at pH 7.4), and passed three times through a French pressure cell at 1500 p.s.i. Cell lysate was centrifuged at 15 000 × *g* to remove unbroken cells and debris and the supernatant was centrifuged at 150 000 × *g* for 1 h to precipitate insoluble material. The soluble fraction was applied to a 1-mL His-Trap nickel affinity column (GE Healthcare) equilibrated with binding buffer (50 mM HEPES, 150 mM NaCl, 10 mM Imidazole, pH 7.4), and His_6-tagged proteins were eluted with a gradient of 0-80% elution buffer (50 mM HEPES, 150 mM NaCl, 500 mM Imidazole, pH 7.4). Proteins were then dialyzed into 50 mM HEPES, 150 mM NaCl, and 10% glycerol, pH 7.4, at 4°C. Protein purity was confirmed using SDS-polyacrylamide gel electrophoresis (see the following section) and 100-μL aliquots were frozen at -80°C.

2.8.2. Protein quantification

Protein concentrations were determined using a Bradford protein assay or spectrophotometric A_{280} assay for experiments and reactions or CD measurements, respectively. Protein yields for rSfaB, rSfaD, and WT or mutant rHtsA were 6.8, 25, and ~50 mg L^{-1}, respectively.

2.8.3. SDS-polyacrylamide gel electrophoresis

Proteins, whole-cell lysates, or resuspended detergent pellets were diluted 3:1 with a protein loading buffer (10% glycerol, 64 mM Tris, 2% SDS, 5% β-mercaptoethanol, and 0.01% bromophenol blue, pH 6.8) and boiled for 10 min prior to SDS-polyacrylamide gel electrophoresis, following standard protocols (127). Briefly, SDS-polyacrylamide gels consisted of a 5% acrylamide (Bio-Rad) stacking gel, 12% acrylamide (Bio-Rad) resolving gel, and were run at 130 V for 1.5 h. Proteins were stained with Coomassie Brilliant Blue R-250 using standard procedures. Gels were then visualized under white light, scanned using a CanoScan LiDE 700F, and illustrated using Adobe Photoshop CS2.

2.9. Western blotting methodologies

2.9.1. *S. aureus* whole cell lysate preparation

S. aureus cells were grown overnight in TMS media, diluted into fresh TMS, and grown for an additional 12 h. The cells were then washed three times with 0.9% w/v saline, equilibrated to an OD_{600} of 1.2, and 100 μL were harvested via centrifugation (10 000 × *g*) for 1 min. The pellets were then resuspended in 100 μL digestion buffer (30% w/v raffinose, 50 mM Tris, 145 mM NaCl, 10 μM phenylmethylsulfonyl fluoride, 50 μg mL^{-1} lysostaphin (Sigma), "pinch" iodoacetamide, and 20 μg mL^{-1} DNAse, pH 7.5) and incubated for 45 minutes at 37°C or until lysis was achieved.

2.9.2. Detergent partitioning of membrane proteins

S. aureus cells were grown overnight in TMS media, diluted into fresh TMS, and grown overnight to late-log-phase. The cells were then harvested by centrifugation (10 000 × *g*), washed three times with 0.9% w/v saline, and equilibrated to an OD_{600} of 1.0 in PBS. The cells were then supplemented with 50 μg mL^{-1} lysostaphin, incubated at 37°C for 15 min, and diluted with 900 μL of PBS. Detergent extraction and phase partitioning was completed as previously described (25). In summary, cells were sonicated twice on a Branson Digital Sonifier® (Branson Ultrasonics Corporation, USA) fitted with a 3-mm-diameter probe, and cooled on ice. 10% v/v Triton X-114 in PBS was then added and each sample was incubated for 2 h at 4°C. Samples were then centrifuged (13 000 × *g*) at 4°C for 10 min to pellet insoluble debris. The supernatants were transferred to clean microcentrifuge tubes, incubated at 37°C for 30 min, and centrifuged (13 000 × *g*) for 10 min at room temperature to pellet the detergent phase. The aqueous phase was then removed and the detergent pellet was washed with 1 mL PBS at 4°C for 1 h, transferred to 37°C for 30 min, repelleted, and diluted 1:1 in deionized water for solubilization.

2.9.3. Generation of anti-HtsA antisera

Rabbit polyclonal antibodies recognizing rHtsA were generated by ProSci (Poway, CA) using custom anti-body production package 1 protocol.

2.9.4. Western Blotting

Following SDS-polyacrylamide electrophoresis, proteins were transferred to a BioTrace™ NT nitrocellulose membrane (Pall Life Sciences) at 250 mA for 1 h. The membranes were then transferred to a clean container, 30 mL of blocking buffer (10% v/v horse serum (Sigma) and 10% w/v skim milk) was added, and they were incubated overnight at 4°C with gentle shaking. Blocking buffer was then removed, 25 mL of a primary antibody solution (1/5000 dilution of primary antisera, 5% v/v horse serum (Sigma), and 2.5% w/v skim milk) was added, and they were incubated for 2 h at 4°C with gentle shaking. The primary antibody solution was then removed and the membranes were washed three times in ~25 mL TBS buffer (20 mM Tris and 150 mM NaCl, pH 7.5) for 10 min. 25 mL of a secondary antibody solution (1/7500 1 mg mL^{-1} anti-rabbit IgG (H&L) (GOAT) Antibody IRDye800® Conjugated (Rockland), 5% v/v horse serum (Sigma), and 2.5% w/v skim milk) was added, and they were incubated for 1 h at 4°C with gentle shaking. The secondary antibody solution was then removed and the membranes were washed three times in ~25 mL of TBS buffer supplemented with 0.05% Tween-20 for 10 min. Membranes were then scanned on a Odyssey Infrared Imager (Li-Cor) and visualized using Odyssey V3.0 software (Li-Cor).

2.10. rHtsA-SA fluorescence spectroscopy

The rHtsA-SA dissociation constant (K_d) was determined using fluorescence spectroscopy as described (58). In summary, fluorescence titration experiments were performed at room temperature using 15 nM rHtsA in 50 mM HEPES, pH 7.4, in a Fluorolog-3 spectrofluorometer (ISA Instruments) across a Fe-SA range of 0.22 and 226 nM. Excitation and emission slits were set at 2.1 and 6.3 nm, respectively, and the excitation and emission wavelengths were set at 280 and 334 nm, respectively. K_d values and relevant parameters were calculated by fitting the fluorescence data to a one-site binding model accounting for ligand depletion and data were analyzed by nonlinear regression analysis using the solver tool add-in from Microsoft Office® Excel software as previously described (134, 135).

2.11. Circular dichroism

Proteins were dialysed into a solution of 10 mM sodium phosphate and 150 mM sodium fluoride, pH 7.4, and normalized to a concentration where the A_{280} was ~0.2. Circular dichroism (CD) measurements were obtained using a J-810 spectropolarimeter (Jasco) with the following settings: standard sensitivity, 260-190 nm measurement range, 0.5 nm data pitch, continuous scanning, 10 nm/min scanning speed, 1 nm bandwidth, and 5 accumulations per sample. Measurements were completed in a 1mm quartz cuvette and data was analyzed using Microsoft Office Excel. The CD signal (θ, in millidegrees) was converted to mean residue ellipticity (MRE) ([θ], in deg·cm^2/dmol) using the equation $[\theta] = \theta \times \text{MRE}/10 \times C \times l$, where MRE = MW/n, prior to graphing.

Chapter 3 - Results

3.1. HtsA has a unique Fe-SA binding pocket

At the start of this project we had just obtained the holo-structure of Fe-SA-rHtsA as illustrated in Figure 5. rHtsA is a class III substrate binding protein and has in common the overall protein fold embodied by other members of this protein family. However, the structure informed us that it used a novel form of ligand entrapment (i.e. many positively charged residues) to bind Fe-SA (58). In order to investigate the Fe-SA-rHtsA binding specificity and affinity, and to meet the objectives as outlined above, I needed to prepare sufficient quantities of Fe-SA and rHtsA.

3.2. *In vitro* synthesis of staphyloferrin A

Near the beginning of my project, Cotton *et al.* demonstrated that SA could be synthesized *in vitro* using recombinant SfaB and SfaD synthetases, along with citric acid and D-ornithine as substrates (27). This confirmed the SA biosynthesis pathway illustrated in Figure 3. For the purposes of my project goals, rSfaB and rSfaD were overexpressed and purified. The purity and integrity of the rSfaB (69.4 kDa) and rSfaD (78.2 kDa) is demonstrated in Figure 7. SA synthesis reactions were set up as described (27). The ion-pair HPLC chromatogram illustrated in Figure 8 demonstrated that only the complete reaction generated a peak that corresponds to Fe-SA (27). Furthermore, CAS shuttle solution (133) was used to quickly assess the iron-binding activity of SA and, in agreement with previous findings, only complete SA synthesis reactions tested positive with CAS shuttle solution (133) (i.e. omitting either enzyme or any reaction component resulted in no siderophore activity).

Figure 7. rSfaB, rSfaD, and rHtsA proteins were purified. Coomassie stained SDS-polyacrylamide gel showing purified his-tagged rSfaB, rSfaD, and rHtsA.

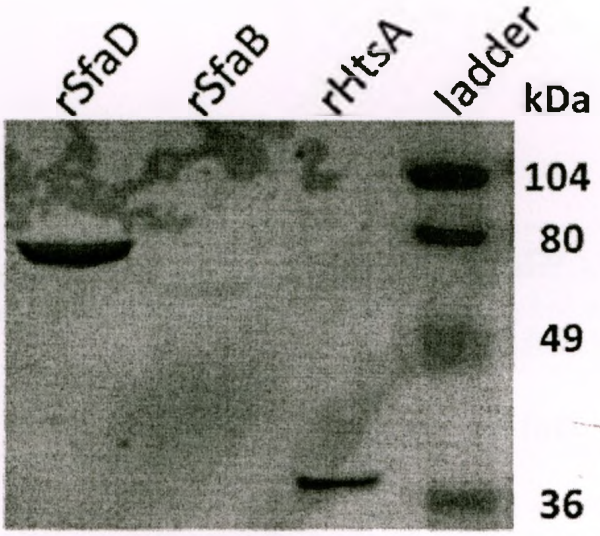
rSfaD
rSfaB
rHtsA
ladder
kDa
104
80
49
36

Figure 8. Ion-pair HPLC analysis of *in vitro* staphyloferrin A production. Missing reaction components are indicated on each trace. Reactions were monitored at 340 nm (see Materials and Methods).

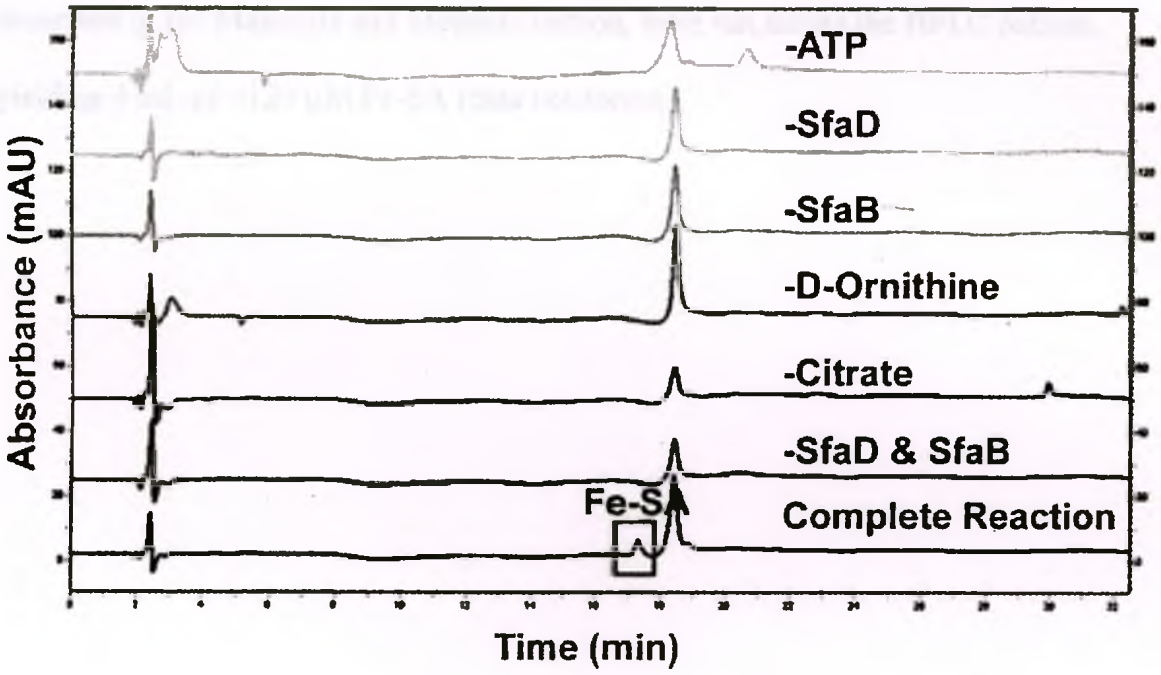
-ATP
-SfaD
-SfaB
-D-Ornithine
-Citrate
-SfaD & SfaB
Complete Reaction
Fe-S
Absorbance (mAU)
Time (min)

SA had to be further purified from the *in vitro* synthesis reactions for use in Fe-SA-rHtsA binding assays. In order to obtain purified Fe-SA, ion-pair HPLC was used to separate the *in vitro* SA synthesis reaction components, and the fractions containing the SA peak were collected (Fig. 9A). LC/MS of the collected fractions and *in vitro* synthesis reactions detected SA at an m/z =479 in both samples, consistent with previous studies (27, 58). As illustrated in Fig. 9B, collection of ion-pair HPLC SA fractions reduces the amount of reaction contaminants present. Eight reaction mixtures, set up as described in the Materials and Methods section, were run across the HPLC column, yielding 4 mL of ~120 μM Fe-SA (data not shown).

Figure 9. Fe-SA can be separated and purified from reaction components using ion-pair HPLC. A) Ion-pair HPLC trace showing the Fe-SA peak eluting at 17.5 min, ahead of reaction components, which elute at 20 min. B) LC/MS demonstrating that Fe-SA fractions are purified from other reaction components. C) LC/MS of unpurified Fe-SA biosynthesis reactions. The reaction was monitored at 340 nm.

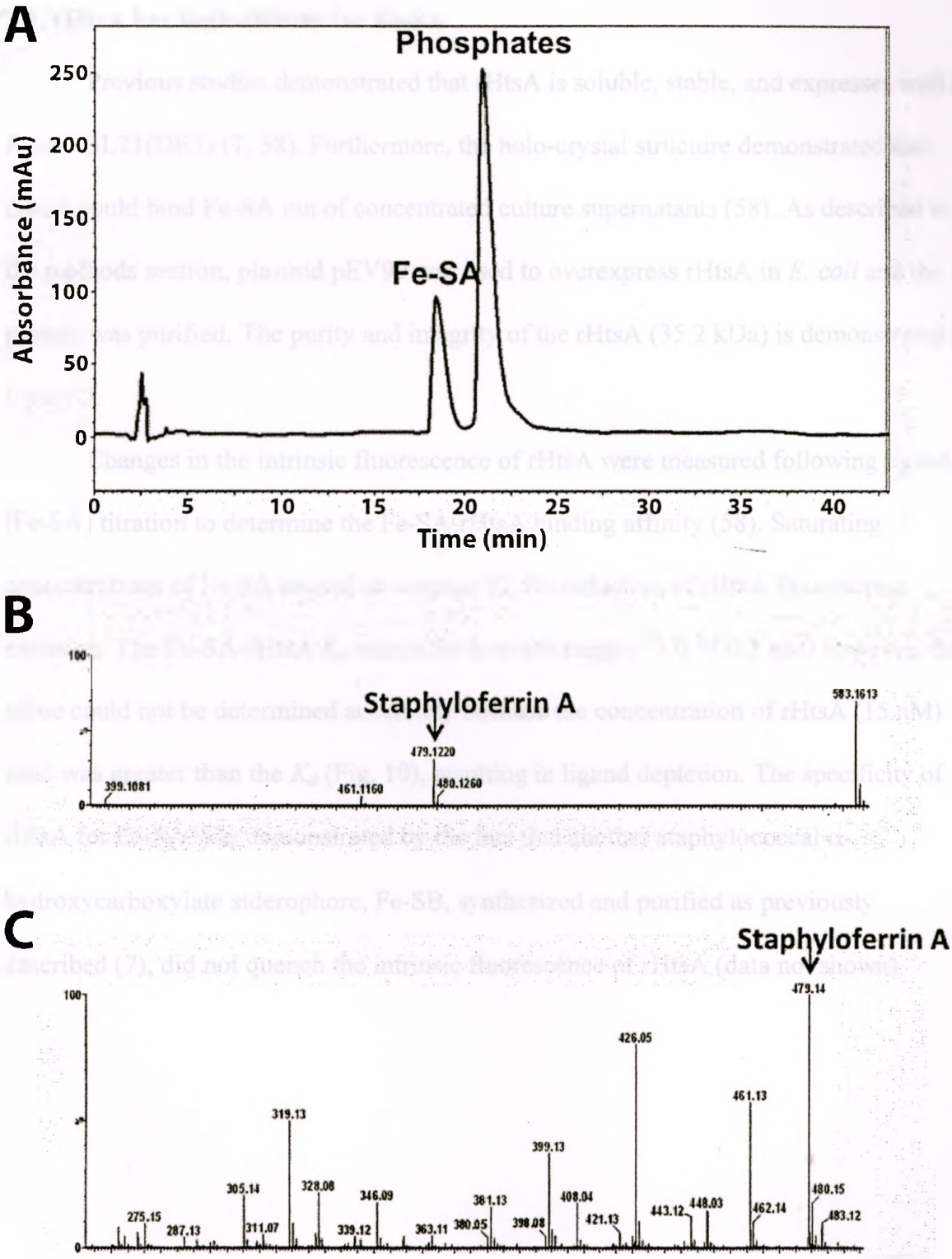
A
Phosphates
Fe-SA
Absorbance (mAu)
250
200
150
100
50
0
0
5
10
15
20
25
30
35
40
Time (min)
B
Staphyloferrin A
583.1613
479.1220
399.1081
461.1160
480.1260
C
Staphyloferrin A
479.14
426.05
461.13
319.13
399.13
305.14
328.08
346.09
381.13
408.04
480.15
275.15
287.13
311.07
339.12
363.11
380.05
398.08
421.13
443.12
448.03
462.14
483.12

3.3. rHtsA has high affinity for Fe-SA

Previous studies demonstrated that rHtsA is soluble, stable, and expresses well in *E. coli* BL21(DE3) (7, 58). Furthermore, the holo-crystal structure demonstrated that rHtsA could bind Fe-SA out of concentrated culture supernatants (58). As described in the methods section, plasmid pEV99 was used to overexpress rHtsA in *E. coli* and the protein was purified. The purity and integrity of the rHtsA (35.2 kDa) is demonstrated in Figure 7.

Changes in the intrinsic fluorescence of rHtsA were measured following ligand (Fe-SA) titration to determine the Fe-SA-rHtsA binding affinity (58). Saturating concentrations of Fe-SA caused an average 52.5% reduction of rHtsA fluorescence emission. The Fe-SA-rHtsA K_d was in the low nM range (~1.0 +/-0.3 nM) however; the value could not be determined accurately because the concentration of rHtsA (15 nM) used was greater than the K_d (Fig. 10), resulting in ligand depletion. The specificity of rHtsA for Fe-SA was demonstrated by the fact that another staphylococcal α-hydroxycarboxylate siderophore, Fe-SB, synthesized and purified as previously described (7), did not quench the intrinsic fluorescence of rHtsA (data not shown).

Figure 10. Saturation curve of the binding of Fe-SA to HtsA. rHtsA was titrated with increasing concentrations (as determined by atomic absorption spectroscopy) of Fe-SA and intrinsic fluorescence knockdown is depicted here as percent saturation. The experimental data is represented as the solid line with diamonds and the theoretical data (predicted by non-linear regression, one-site binding model) is the dashed line. Inset represents an emphasis in the region of Fe-SA concentrations used to determine the dissociation constant. Data is the result of three independent experiments using different batches of HtsA and error bars represent standard deviation from the mean.

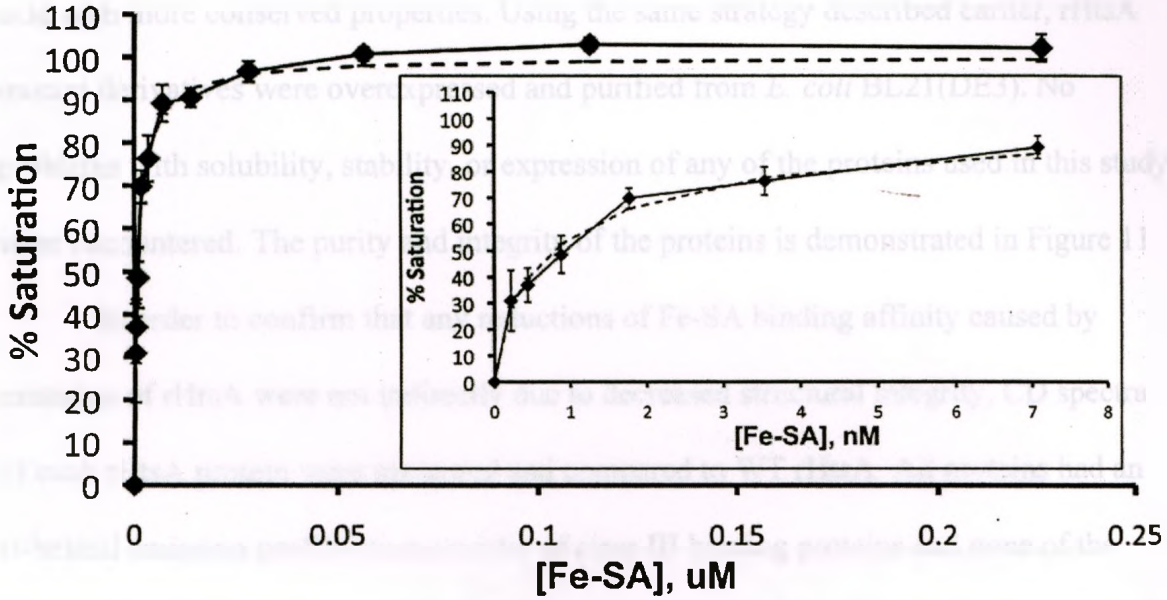
% Saturation
[Fe-SA], uM
0
10
20
30
40
50
60
70
80
90
100
110
0
0.05
0.1
0.15
0.2
0.25
% Saturation
[Fe-SA], nM
0
1
2
3
4
5
6
7
8

3.4. Amino acid substitutions do not affect overall protein fold of rHtsA

The Fe-SA-rHtsA crystal structure identified several rHtsA residues that formed contacts with Fe-SA (Fig. 5C). As outlined in the objectives, one of my goals was to determine the significance of those residues for productive binding *in vitro*. To investigate the role of each residue found to interact with SA, site-directed mutagenesis on pEV99 was used to substitute each interacting residue with either alanine or an amino acid with more conserved properties. Using the same strategy described earlier, rHtsA mutant derivatives were overexpressed and purified from *E. coli* BL21(DE3). No problems with solubility, stability, or expression of any of the proteins used in this study were encountered. The purity and integrity of the proteins is demonstrated in Figure 11.

In order to confirm that any reductions of Fe-SA binding affinity caused by mutation of rHtsA were not indirectly due to decreased structural integrity, CD spectra of each rHtsA protein were measured and compared to WT rHtsA. All proteins had an α-helical emission profile characteristic of class III binding proteins and none of the mutations I constructed in rHtsA resulted in any significant difference in the CD spectra compared to WT protein (Fig. 12).

Figure 11. WT and mutant rHtsA proteins were purified. Coomassie stained SDS-polyacrylamide gel showing purified his-tagged WT and mutant rHtsA.

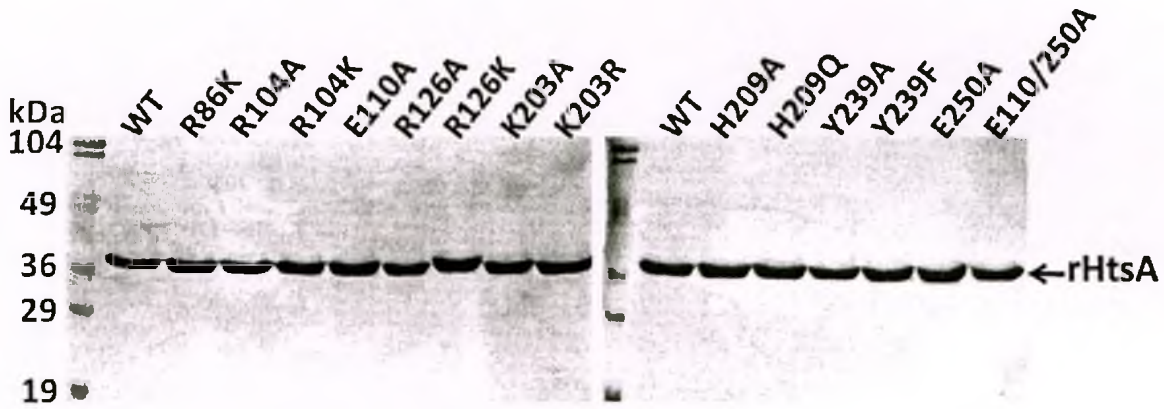
kDa
104
49
36
29
19
WT
R86K
R104A
R104K
E110A
R126A
R126K
K203A
K203R
WT
H209A
H209Q
Y239A
Y239F
E250A
E110/250A
←rHtsA

Figure 12. Point mutations do not result in gross rHtsA conformational changes. Circular dichroism spectra of WT and mutant rHtsA proteins indicate a proper α-helical conformation. Spectra were analyzed across wavelengths of 260 to 190 nm. MRE, mean residue ellipticity.

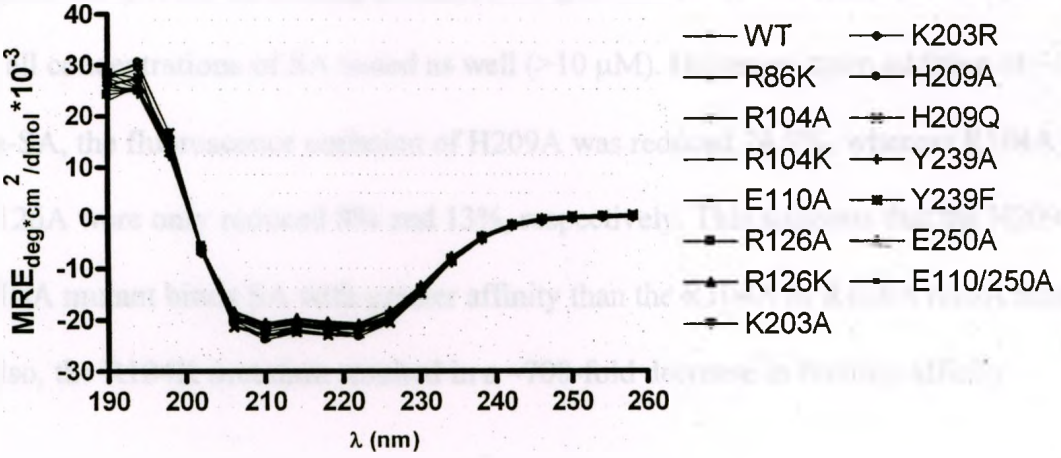
40
30
20
10
0
-10
-20
-30
190
200
210
220
230
240
250
260
λ (nm)
MRE deg*cm 2 /dmol *10-3
WT
R86K
R104A
R104K
E110A
R126A
R126K
K203A
K203R
H209A
H209Q
Y239A
Y239F
E250A
E110/250A

3.5. HtsA R104A, R126A, and H209A have reduced Fe-SA-rHtsA binding affinity

Using the approach described earlier, the effect that each mutation had on the Fe-SA-rHtsA K_d was determined (Table 6). R104A and R126A mutations resulted in the greatest reductions of binding affinity, failing to reach saturating levels of rHtsA fluorescence quenching at all concentrations of SA tested (>1.3 μM). H209A also had a significantly reduced binding affinity, failing to saturate rHtsA fluorescence quenching at all concentrations of SA tested as well (>10 μM). However, upon addition of ~1.2 μM Fe-SA, the fluorescence emission of H209A was reduced 24.9%, whereas R104A and R126A were only reduced 8% and 13%, respectively. This suggests that the H209A rHtsA mutant binds SA with greater affinity than the R104A or R126A rHtsA mutants. Also, the R104K mutation resulted in a ~700-fold decrease in binding affinity.

Table 6. Effect of rHtsA mutations on binding affinity

Protein (rHtsA)	Ligand[a]	Dissociation Constant (K_d)[b]
WT	Fe-SA	0.91±0.34 nM
WT	Fe-SB	DNB[c]
R86K	Fe-SA	1.37±0.42 nM
R104A	Fe-SA	DNB[c]
R104K	Fe-SA	723±231 nM
E110A	Fe-SA	ND[d]
R126A	Fe-SA	DNB[c]
R126K	Fe-SA	1.00±0.03 nM
K203A	Fe-SA	5.23±2.19 nM
K203R	Fe-SA	5.07±1.11 nM
H209A	Fe-SA	DNB[c]
H209Q	Fe-SA	2.01±0.23 nM
Y239A	Fe-SA	2.36±0.11 nM
Y239F	Fe-SA	2.60±0.02 nM
E250A	Fe-SA	1.18±0.17 nM
E110/250A	Fe-SA	ND[d]

[a] Ligands are ferrated prior fluorescence titrations.

[b] Values represent averages and ± denotes standard deviation, n=3.

[c] DNB, does not bind; no fluorescence saturation when [siderophore] > 1 μM.

[d] ND, not determined.

3.6. HtsABC is required for Fe-SA uptake

Previously, Beasley *et al.* demonstrated that HtsABC is required for the transport of Fe-SA using two separate assays (7). Additionally, it was demonstrated that chromosomal deletion of *htsABC* in *S. aureus* Newman in the absence of Fe-SB uptake results in a drastic reduction of growth under iron-restricted conditions (7). Using similar strategies, one of my major objectives was to determine the significance of each HtsA residue identified earlier for productive transport *in vivo*.

In order to do this, I first needed a vector that could complement the *S. aureus* Newman Δ*htsABC* associated growth reduction. Importantly, Beasley *et al.* also demonstrated that growth could be rescued via complementation with pEV55, an *E. coli*/*S. aureus* shuttle vector containing the *S. aureus htsABC* operon and promoter region (7). To investigate the role of each residue found to interact with SA *in vivo*, site-directed mutagenesis on pEV55 was used to substitute each interacting residue with either alanine or an amino acid with more conserved properties.

3.7. *S. aureus* expresses recombinant HtsABC

Although previous studies demonstrated that plasmid-borne HtsABC could complement *S. aureus* Newman Δ*htsABC*, I needed to confirm proper expression of the mutant derivatives of HtsA. In order to verify this, Western immunoblots against HtsA were completed in whole cell lysates of *S. aureus* Newman Δ*htsABC* harboring WT or mutant pEV55. As illustrated in Figure 13, all pEV55 constructs resulted in similar HtsA expression levels.

Figure 13. WT and mutant HtsA express well in *S. aureus* Newman. Western immunoblots using anti-HtsA antiserum were completed on whole-cell lysates of *S. aureus* Newman. WT and mutant derivatives express similar amounts of HtsA. No HtsA is detected in the *S. aureus* mutant carrying empty vector.

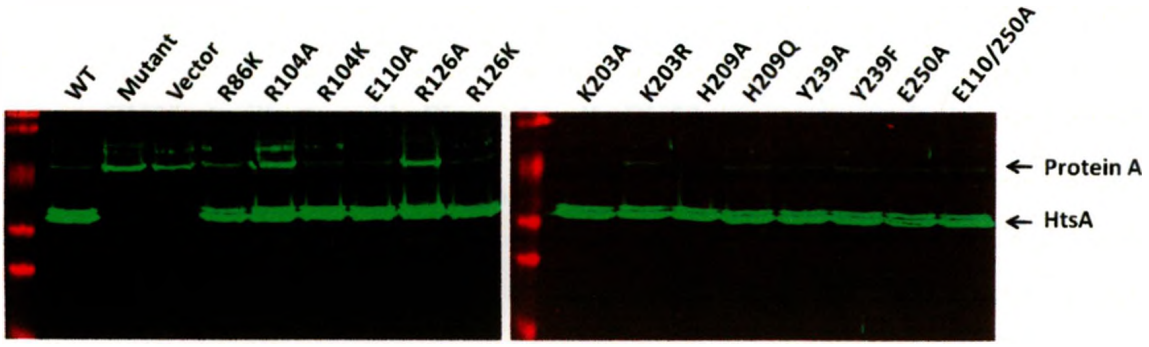
WT
Mutant
Vector
R86K
R104A
R104K
E110A
R126A
R126K
K203A
K203R
H209A
H209Q
Y239A
Y239F
E250A
E110/250A
Protein A
HtsA

3.8. *S. aureus* HtsA localizes to the extracellular membrane

HtsA is a class III substrate binding protein that is tethered to the extracellular face of the cytoplasmic membrane via N-terminal lipidation. There, it functions as the Fe-SA-receptor before docking to its cognate permeases, HtsBC. In order to confirm that any growth deficits caused by mutation of HtsA were not indirectly due to altered protein expression and/or localization, Western immunoblots against HtsA were completed in detergent extracted membrane fractions of *S. aureus* harboring WT or mutant pEV55. As illustrated in Figure 14, all pEV55 constructs resulted in expression of HtsA that was localized to the cytoplasmic membrane.

Figure 14. WT and mutant HtsA localize to the cell membrane of *S. aureus* Newman. Western immunoblots using anti-HtsA antiserum were completed on detergent extracted membrane fractions from *S. aureus* Newman. No HtsA is detected in the *S. aureus* mutant carrying empty vector.

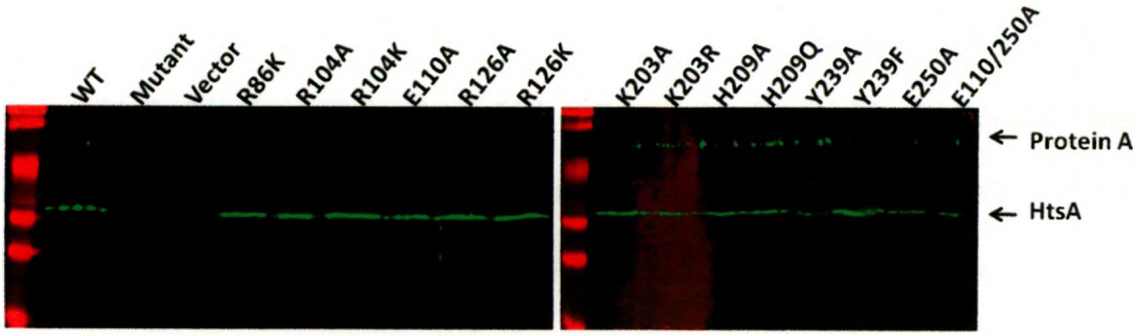
WT
Mutant
Vector
R86K
R104A
R104K
E110A
R126A
R126K
K203A
K203R
H209A
H209Q
Y239A
Y239F
E250A
E110/250A
Protein A
HtsA

3.9. Substitution of HtsA R104A, R126A, or H209A reduces Fe-SA-dependant growth of *S. aureus* in iron-restricted liquid growth media

In order to determine the significance of each HtsA residue substitution for productive transport *in vivo*, I generated iron-restricted growth curves of *S. aureus* Newman Δ*htsABC* harboring WT or mutant derivatives of pEV55. As illustrated in Figure 15, substitution of HtsA R104A or R126A resulted in drastic growth reductions and substitution of HtsA H209A severely delayed growth. Importantly, these results agree with the binding affinity data which indicated that HtsA with substitutions R104A, R126A and H209A had severe reduction in ligand binding. Interestingly, although HtsA R104K had a 700-fold higher K_d for Fe-SA than WT HtsA, *S. aureus* harbouring this HtsA mutation was not debilitated for SA-dependent growth. All growth deficits were rescued by the addition of 50 μM $FeCl_3$, a growth condition that eliminates the requirement for Fe-SA for growth.

Figure 15. Identification of HtsA mutations that impair SA-dependant growth of *S. aureus*. *S. aureus* expressing HtsA R104A, R126A, or H209A are impaired for SA-dependent growth. Inset, growth of all strains is restored with the addition of 50 μM $FeCl_3$, thus eliminating the requirement for Fe-SA iron for growth. Growth is in 80% horse serum (Sigma) and 20% Chelex®-treated TMS. Error bars represent standard deviation, $n = 3$.

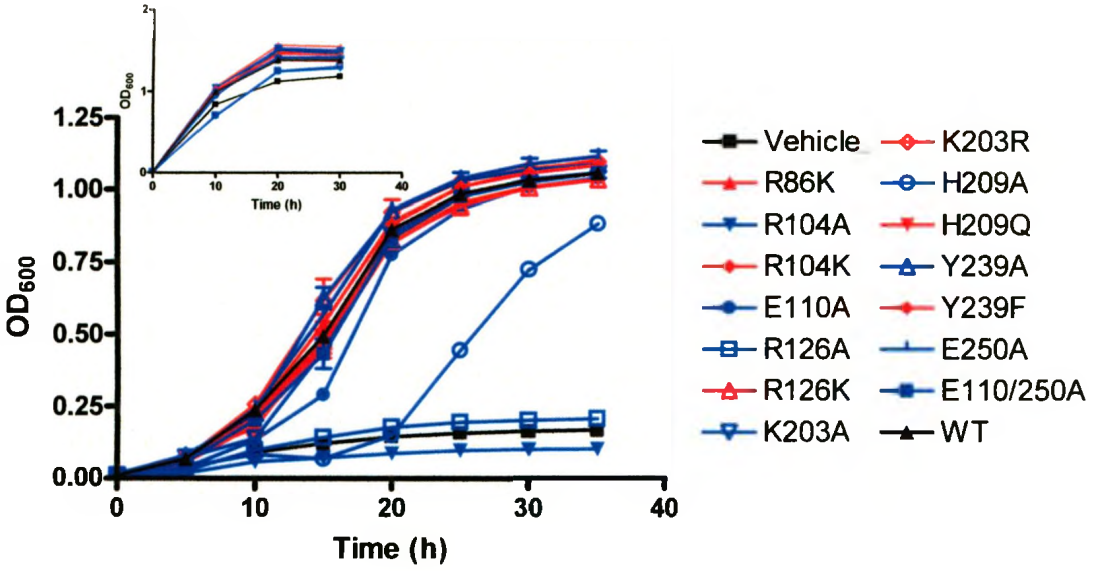
OD600
1.25
1.00
0.75
0.50
0.25
0.00
0
10
20
30
40
Time (h)
Vehicle
R86K
R104A
R104K
E110A
R126A
R126K
K203A
K203R
H209A
H209Q
Y239A
Y239F
E250A
E110/250A
WT

3.10. An alternate growth assay identifies that HtsA R86K, R104A, R126A, R126K, K203A, H209A, H209Q, Y239A, and E110/250A mutants are impaired for Fe-SA-dependent growth of *S. aureus*

Beasley *et al.* used disk diffusion assays, in addition to the liquid culture growth curves, to further demonstrate the role of HtsABC in Fe-SA uptake (7). I used this assay in an attempt to gain more insight into the role of HtsABC in SA-dependent growth. Thus, disk-diffusion assays were completed for *S. aureus* Newman Δ*htsABC* harboring WT or mutant pEV55, using purified Fe-SA that was spotted onto the bacteria-containing media. As illustrated in Figure 16, substitution of either HtsA R104A or R126A completely abolished Fe-SA-dependant growth and substitution of HtsA H209A significantly reduced Fe-SA-dependant growth. However, as opposed to the liquid growth assay, this assay identified that substitution of HtsA R86K, R126K, K203A, H209Q, Y239A, and E110/250A also significantly reduced Fe-SA-dependent growth. However, growth reductions associated with these additional residues were more moderate. Importantly, this trend agrees with the binding affinity data. As a control, I showed that no growth differences were observed when Fe-Desferal™ was used as the iron source, demonstrating that the growth reductions observed were specific for Fe-SA.

Figure 16. Plate disk-diffusion growth assay confirms HtsA mutations that impair SA-dependant growth of *S. aureus*. Growth promotion is measured as the diameter (mm) of growth around each disk. The dashed line indicates the diameter of each disk and a measurement of 6 mm indicates no growth. In panel A, Fe-SA is added as the sole iron source, whereas in panel B, Fe-Desferal™ is added as the sole iron source. Error bars represent standard deviation, $n = 3$. Statistical significance is determined for each mutant in comparison to WT. [a] P=<0.0001. [b] P=<0.001. [c] P=<0.05.

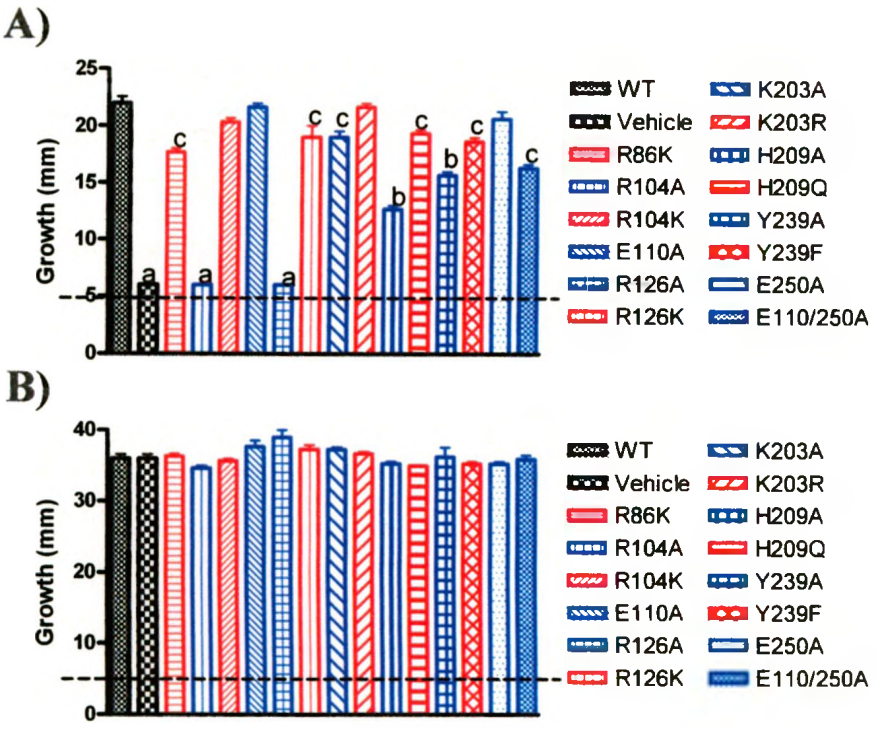
A)
Growth (mm)
25
20
15
10
5
0
a
c
a
c
c
a
c
b
c
b
c
c
WT
Vehicle
R86K
R104A
R104K
E110A
R126A
R126K
K203A
K203R
H209A
H209Q
Y239A
Y239F
E250A
E110/250A
B)
Growth (mm)
40
30
20
10
0
WT
Vehicle
R86K
R104A
R104K
E110A
R126A
R126K
K203A
K203R
H209A
H209Q
Y239A
Y239F
E250A
E110/250A

Chapter 4 - Discussion

Bacterial pathogens must have the ability to scavenge host iron in order to establish and maintain productive infections. *S. aureus* is one of the most successful human pathogens, partly due to its enormous virulence factor repertoire and multiple host iron-scavenging systems. Indeed, studies have demonstrated that disruption of staphyloferrin B biosynthesis reduces *S. aureus* pathogenesis in a mouse model of infection (32). Two staphylococcal siderophore systems have been genetically and biologically characterized. The *sfa* and *hts* loci encode the SA biosynthesis machinery (27) and ABC-transporter (7), respectively, and the *sbn* and *sir* operons encode the SB biosynthesis machinery and ABC-transporter, respectively (32). Recently, our laboratory, along with collaborators, published crystal structures of Fe-SA-rHtsA and Fe-SB-rSirA (58, 57). HtsA was the first Gram-positive α-hydroxycarboxylate siderophore receptor crystal structure. Although both SA and SB are anionic α-hydroxycarboxylate siderophores, each receptor is specific for its cognate siderophore (58, 57). The *hts* system is present ubiquitously among the chromosomes of sequenced *Staphylococci* making it an ideal candidate for binding affinity and biological studies in order to establish a model system of staphylococcal siderophore uptake.

The *sfa* locus was identified via bioinformatics searches and consists of genes expressing two NIS synthetases, an exporter, and a PLP-dependant ornithine racemase (27). The gene cluster is Fur regulated and is responsible for the synthesis and secretion of SA (27). It is present in all sequenced Staphylococcal chromosomes, including clinically relevant CoNS (7). SA has been isolated from culture supernatants of *S. hyicus* and chemically characterized (80). More recently, the biosynthesis pathway of SA has

been elucidated and it has been synthesized *in vitro* using rSfaB and rSfaD. One of the first objectives of this study was to purify sufficient amounts of Fe-SA from *in vitro* synthesis reactions.

Using the ion-pair HPLC strategy previously described, I separated Fe-SA from reaction components and collected the fractions that corresponded to the Fe-SA peak (27). This further purified the Fe-SA, a necessary step for its use in binding affinity assays (58). Although CAS shuttle solution (133) has been used to normalize SA siderophore units, it cannot be used to quantify the ion-pair HPLC fractions because they were ferrated prior to injection onto the column (7). Therefore, I chose an indirect approach to quantify the Fe-SA by using AAS to measure the amount of iron bound to SA in the samples. With the known siderophore to iron binding ratio of 1:1, I determined the amount of Fe-SA present (58). This yielded sufficient amounts of Fe-SA for use in experiments (~120 μM).

The *hts* operon is located adjacent to the *sfa* locus and is also present in the chromosomes of all sequenced staphylococci (7). It encodes a lipoprotein receptor and two permeases that are necessary for Fe-SA transport (7). However, the *hts* operon was first implicated in heme uptake following the observation that transposon disruption of *hts* resulted in preferential uptake of transferrin Fe(III) over heme Fe(II) (137). This phenomenon may be explained by a dual role of heme and Fe-SA uptake by the HtsBC permeases (7). Indeed, Cuiv *et al.* demonstrated that a *Sinorhizobium meliloti* 2011 permease is involved in heme and hydroxamate siderophore uptake (31). However, it is unlikely that HtsA functions as a heme binding protein, as the crystal structure of Fe-

SA-rHtsA identifies Fe-SA in a highly positively charged binding pocket that is more suitable for an anionic siderophore than a hydrophobic heme molecule (58).

One of the first major objectives of this study was to determine the binding affinity of HtsA for Fe-SA. This information would allow better comparisons with related proteins, provide insight on the mechanism of ligand binding, and further clarify the role of HtsA in Fe-SA transport. Using the purified Fe-SA and rHtsA I determined the K_d value of Fe-SA-rHtsA to be in the low nM range (58). This was the first determination of the affinity between an α-hydroxycarboxylate siderophore and its receptor (58). The strength of the affinity was not surprising considering that rHtsA complexed and crystallized with Fe-SA when exposed to ferrated *S. aureus* culture supernatant (58). The number of ionic contact points that rHtsA makes with Fe-SA in combination with the envelopment of Fe-SA in the binding pocket likely explains the high affinity. Furthermore, the affinity of rSirA for Fe-SB, another α-hydroxycarboxylate siderophore-receptor complex, has recently been published and is within the same range (57). Both affinities are within the range of several Gram-negative bacteria outer membrane receptors for their respective ligands but they are significantly greater than the affinity of *E. coli* FhuD (Table 1). The high affinities of HtsA and SirA for Fe-SA and Fe-SB, respectively, are likely due to the number and type of ionic interactions involved in siderophore co-ordination (58, 57). However, the significant difference in their affinities compared to FhuD is likely accounted for by their ligand repertoire. Indeed, whereas HtsA and SirA are specific for Fe-SA and Fe-SB, respectively (58, 57), FhuD binds a broad range of Fe-hydroxamate siderophores (122), and likely sacrifices affinity for broadened substrate specificity.

Unique open and closed ligand-bound conformations allowed identification and characterization of a novel form of ligand entrapment for a class III binding protein (58). Many crystal structures of related proteins, such as BtuF (10, 78), TroA (86, 87), FhuD (24, 82), and ShuT (67) have similar structural folds but little, if any, conformational changes between apo and holo forms. Although FitE (136) and FeuA (112) both undergo larger hinged movements more reminiscent of HtsA, their conformational changes are characterized by rigid interdomain movement, whereas HtsA conformational changes occur in isolated regions of the C-terminal domain (58). In addition, the unique HtsA movements help occlude SA by shifting it deeper in the binding pocket, reducing solvent exposure, and facilitating additional contact points (58). Only SirA has been demonstrated to have similar C-terminal domain movements however, the conformational changes, siderophore orientation, and receptor residues involved in coordination are distinct and each receptor is specific for its cognate siderophore (58, 57).

One of the major objectives of this study was to identify and mutate what were thought at the outset to be HtsA residues critical for Fe-SA interaction. Analysis of the crystal structure identified many potential residues and I initially selected six amino acids that form H-bonds with Fe-SA, R86, R104, R126, K203, H209, and Y239, and two residues predicted to form salt-bridges that mediate docking with the permeases, HtsBC, E110 and E250 (58). In Grigg, Cooper, *et al.*, we aligned 41 homologous sequences of HtsA which showed that the residues selected were conserved to varying degrees, R86, 22/41; R104, 37/41; R126, 36/41; H209, 30/41; Y239, 9/41; E110, 39/41; and E250, 38/41 (58). I created alanine amino acid substitutions of each residue as well as less

drastic amino acid substitutions that aimed to conserve size, charge, or ring structure. My studies focused on the contribution of each residue to productive SA binding or transport. Before assessing their roles I confirmed that all mutant rHtsA could be expressed, purified, and properly folded from *E. coli*. I also confirmed that they express properly in *S. aureus* and localize to the cellular membrane.

To assess each residue's importance for Fe-SA binding, I determined the effect that each substitution had on the Fe-SA-rHtsA binding affinity. The four residue substitutions that had the most drastic reductions of binding affinity were HtsA R104A, R126A, R126K and H209A. Interestingly, R104, R126, and H209 are the only residues investigated that form contacts with Fe-SA in both open and closed conformations of HtsA. This highlights the importance of the initial contacts made in the open conformation for Fe-SA binding. The R104 and R126 residues are also the most highly conserved of the selected residues that form contacts with Fe-SA and their importance for binding likely explains their degree of conservation. Furthermore, reintroduction of a positive charge via R104K substitution rescued Fe-SA-rHtsA binding, whereas R126K substitution did not. Therefore, the charge on residue R104 is likely the most important factor for productive binding, but the charge and position of residue R126 are both important. Substitution of H209A also eliminated measureable Fe-SA-rHtsA binding. Interestingly, H209 is the third most conserved residue and substitution of H209Q re-established the low nM binding affinity of Fe-SA-rHtsA. This likely indicates an atom capable of H-bonding (nitrogen in this case) is necessary and sufficient for binding at residue H209. As expected, substitution of HtsA E250A, that is located outside of the binding pocket and predicted to be involved in docking with HtsBC, did not change the

Fe-SA-rHtsA binding affinity. More surprising however is that substitution of HtsA K203A and Y239A, which are both involved in H-bonding with Fe-SA in the closed conformation, did not affect the Fe-SA-rHtsA binding affinity. It was especially interesting that the HtsA Y239A substitution did not elicit a pronounced effect because it moved 12.1 Å between the open and closed conformations before H-bonding and enveloping Fe-SA in the binding pocket. Taken together, these results may indicate that the contacts formed in the open conformation are the most important for binding, whereas the contacts formed in the closed conformation may have more important roles in the selectivity of HtsA.

Another major focus of this research was to determine the significance that each residue has on iron-restricted SA-dependant growth of *S. aureus* Newman. Interestingly, the impact each HtsA residue substitution had on growth under these conditions mirrored their effect observed on the Fe-SA-rHtsA binding affinity. Substitution of HtsA R104A or R126A severely reduced *S. aureus* Newman growth. The binding affinity data suggests that this was likely due to their inability to facilitate Fe-SA binding. However, the ~700-fold reduction in binding affinity observed following substitution of HtsA R126K did not confer a measureable growth defect. Two possible explanations may account for this finding. First, pEV55 is a multi-copy vector and the subsequent increase in HtsA expression may have compensated for the decreased binding affinity and secondly, an ~700 nM K_d is still within the affinity range observed for FhuD and therefore, may not sufficiently compromise Fe-SA-HtsA binding and transport. Substitution of HtsA H209A severely delayed but did not eliminate growth. It is possible that the reduction of growth was not as severe as seen for the substitutions of HtsA

R104A or R126A because it was still able to bind Fe-SA sufficiently for transport. Although the K_ds of HtsA R104A, R126A, and H209A were not determined, the titration of HtsA H209A with Fe-SA resulted and a greater reduction of the intrinsic fluorescence which may indicate better binding (data not shown). Together with the lack of a growth phenotype observed for the R126K substitution, substitution of HtsA H209A likely permits sufficient Fe-SA binding to promote growth once enough HtsA is expressed, explaining the delay. Unlike the Fe-SA-rHtsA binding affinity, substitution of HtsA E110/250A was expected to prevent docking of HtsA to HtsBC and therefore, prevent transport of Fe-SA and growth under iron-restricted Fe-SA-dependant conditions. However, no growth phenotype for HtsA E110/250A was observed. This will be examined in more detail below. Also, once again substitution of HtsA K203A or Y239A did not affect the proper function of HtsA, as there was no observable growth phenotype for either substitution. This further suggests that the additional Fe-SA-HtsA contacts formed in the closed conformation of HtsA have a more significant role in ligand specificity than for productive binding and transport. This will be addressed in more detail in the future directions section of this thesis.

Finally, the last focus of my research was to use a disk diffusion assay as previously described, to further examine the significance that each residue has on Fe-SA-dependent growth promotion of *S. aureus* Newman. Importantly, the HtsA residue substitutions resulted in the same trend observed for growth promotion as seen in the growth curves and Fe-SA-rHtsA binding affinities. However, the disk-diffusion growth assay appeared to be more sensitive than the liquid growth assay. A possible explanation for the assay's increased sensitivity is the higher degree of iron restriction (7.5 μM

EDDHA) used in the growth media. In addition to the HtsA substitutions identified in the previous experiments, the substitution of HtsA R86K, R126K, K203A, H209Q, Y239A, Y239F and E110/250A, resulted in significantly reduced growth promotion, albeit to a lesser degree than substitution of HtsA R104A, R126A, and H209A. Interestingly, substitution of HtsA R104K did not result in a significant growth phenotype and substitution of HtsA R126K only resulted in a modest growth reduction that was comparable to the growth reductions observed following substitution of HtsA R86K, K203A, H209Q, Y239F and E110/250A. These proteins did not result in decreased Fe-SA binding affinities however, this may be due to the reductions being too subtle to detect with the concentration of HtsA used in the fluorescence titrations. Lower protein concentrations may result in more accurate K_ds that reflect the same trend observed for the growth reductions.

Although the results concerning the substitution of some of the HtsA residues involved in Fe-SA binding were expected, two very surprising findings of this study was the ability of the E110/250A mutant derivative to facilitate productive transport of Fe-SA and the ability of the Y239A mutant derivative to facilitate productive binding and transport of Fe-SA. This was surprising because HtsA E110 and E250 are both highly conserved (39/41 and 38/41, respectively) based on alignment of homologous HtsA sequences, and modeling of HtsBC with the Fe-SA-rHtsA crystal structure predicted that they are involved in Glu-Arg salt-bridge formation between the receptor and membrane transporter (58). More importantly, similar salt-bridge formation and subsequent docking with their cognate ABC-transporter is necessary for productive transport in related proteins, including *E. coli* FecB (12) and *S. aureus* FhuD2 (134). However, my

data suggest that the HtsBC permeases may be less reliant on those residues than FecB or FhuD2 for docking of receptor and permease, or simply that the levels of SA-dependent growth observed in my assays due to high levels of multicopy HtsABC overshadowed any defects due to absence of the salt-bridge formation. As mentioned earlier, the absence of an effect of substitution of HtsA Y239A on productive binding or transport was also peculiar. Analysis of the open and closed forms of the Fe-SA-rHtsA crystal structure revealed that Y239 traversed the binding pocket before H-bonding and securing Fe-SA in the binding pocket. Furthermore, Y239 moves 12.1 Å, the furthest of any HtsA residue, and is part of an eight amino acid insertion that absent from all homologous sequences (58). My data suggest that HtsA Y239 does not have a major role in productive binding or transport of Fe-SA however, its role in the specificity of HtsA for Fe-SA warrants further investigation.

In summary, I have determined the first K_d of an α-hydroxycarboxylate siderophore and its receptor, developed a method of purifying and quantifying useful quantities of Fe-SA from *in vitro* synthesis reactions, and analyzed and confirmed the contribution of several amino acid residues identified from the Fe-SA-rHtsA crystal structure. My methods will allow Fe-SA to be readily available for use in future experiments and my results have clarified some of the conclusions drawn from analysis of the crystal structure. For example, substitution of HtsA R104A, R126A, and H209A confirmed the importance of the residues that bind Fe-SA in the open conformation but substitution of HtsA Y239A and E110/250A demonstrated the importance of verifying conclusions drawn from analysis of a crystal structure or from comparison with homologous proteins. Additionally, determination of the Fe-SA-rHtsA K_d has facilitated

comparison of HtsA with related class III binding proteins and Gram-negative outer membrane receptor proteins.

Future Directions

My research has increased the understanding of *S. aureus* SA binding and transport, the first such study involving a receptor protein for a polycarboxylate siderophore. Moreover, through this work I have also provided tools (purified and quantified Fe-SA) that can be used to facilitate greater knowledge of the staphylococcal *sfa-hts* system, including the generation of additional sets of mutations in *htsA* and even *htsBC*. One of the most interesting avenues of research that remains to be studied is investigation of the importance of SA-mediated iron uptake in CoNS. There is no iron-restricted growth defect associated with the loss of *sfa* or *hts* in *S. aureus*, due to the presence of the *sbn-sir*-encoded SB iron uptake system. However, this latter system is absent from all sequenced chromosomes of CoNS (7) and, therefore, in these organisms, the *sfa-hts* system may take on a more prominent role in iron acquisition and potentially virulence. Additionally, the contribution of HtsABC to heme uptake has yet to be resolved. Thorough analysis of *htsA* and *htsBC* mutants or the identification of an additional lipoprotein involved in heme uptake would clarify the role of the *hts* system in staphylococci and significantly improve our understanding of *S. aureus* host iron-uptake strategies. Also, because my results demonstrated the importance of verifying conclusions drawn from a crystal structure, further investigations into the roles of the residues that have been identified in the Fe-SB-rSirA crystal structure are warranted.

References

1. **Archibald, F.** 1983. *Lactobacillus plantarum*, an organism not requiring iron. FEMS Microbiol. Rev. **19:**29-32.
2. **Allen, C. E. and M. P. Schmitt.** 2009. HtaA is an iron-regulated hemin binding protein involved in the utilization of heme iron in *Corynebacterium diphtheriae*. J. Bacteriol. **191:**2638-2648.
3. **Anderson, G. J., A. Dancis, D. G. Roman, and R. D. Klausner.** 1994. Ferric iron reduction and iron uptake in eucaryotes: studies with the yeasts *Saccharomyces cerevisiae* and *Schizosaccharomyces pombe*. Adv. Exp. Med. Biol. **356:**81-89.
4. **Andrews, S. C., A. K. Robinson, and F. Rodriguez-Quinones.** 2003. Bacterial iron homeostasis. FEMS Microbiol. Rev. **27:**215-237.
5. **Beasley, F. C. and D. E. Heinrichs.** 2010. Siderophore-mediated iron acquisition in the staphylococci. J. Inorg. Biochem. **104:**282-288.
6. **Beasley, F. C., C. L. Marolda, J. Cheung, S. Buac, and D. E. Heinrichs.** 2011. *Staphylococcus aureus* transporters Hts, Sir and Sst capture iron liberated from human transferrin by staphyloferrin A, staphyloferrin B and catecholamine stress hormones, respectively, and contribute to virulence. Infect. Immun.
7. **Beasley, F. C., E. D. Vines, J. C. Grigg, Q. Zheng, S. Liu, G. A. Lajoie, M. E. Murphy, and D. E. Heinrichs.** 2009. Characterization of staphyloferrin A biosynthetic and transport mutants in *Staphylococcus aureus*. Mol. Microbiol. **72:**947-963.
8. **Bhakdi, S. and J. Tranum-Jensen.** 1991. Alpha-toxin of *Staphylococcus aureus*. Microbiol. Rev. **55:**733-751.
9. **Bhatt, G. and T. P. Denny.** 2004. *Ralstonia solanacearum* iron scavenging by the siderophore staphyloferrin B is controlled by PhcA, the global virulence regulator. J. Bacteriol. **186:**7896-7904.
10. **Borths, E. L., K. P. Locher, A. T. Lee, and D. C. Rees.** 2002. The structure of *Escherichia coli* BtuF and binding to its cognate ATP binding cassette transporter. Proc. Natl. Acad. Sci. U. S. A. **99:**16642-16647.
11. **Boyer, E., I. Bergevin, D. Malo, P. Gros, and M. F. Cellier.** 2002. Acquisition of Mn(II) in addition to Fe(II) is required for full virulence of *Salmonella enterica* serovar *Typhimurium*. Infect. Immun. **70:**6032-6042.
12. **Braun, V. and C. Herrmann.** 2007. Docking of the periplasmic FecB binding protein to the FecCD transmembrane proteins in the ferric citrate transport system of *Escherichia coli*. J. Bacteriol. **189:**6913-6918.
13. **Braun, V. and M. Braun.** 2002. Active transport of iron and siderophore antibiotics. Curr. Opin. Microbiol. **5:**194-201.
14. **Braun, V., M. Braun, and H. Killmann.** 2000. Iron transport in *Escherichia coli*. Crystal structure of FhuA, an outer membrane iron and antibiotic transporter. Adv. Exp. Med. Biol. **485:**33-43.
15. **Braun, V., K. Hantke, and W. Koster.** 1998. Bacterial iron transport: mechanisms, genetics, and regulation. Met. Ions Biol. Syst. **35:**67-145.

16. **Bronner, S., H. Monteil, and G. Prevost.** 2004. Regulation of virulence determinants in *Staphylococcus aureus*: complexity and applications. FEMS Microbiol. Rev. **28:**183-200.
17. **Chakraborty, T., M. Leimeister-Wachter, E. Domann, M. Hartl, W. Goebel, T. Nichterlein, and S. Notermans.** 1992. Coordinate regulation of virulence genes in Listeria monocytogenes requires the product of the prfA gene. J. Bacteriol. **174:**568-574.
18. **Challis, G. L.** 2005. A widely distributed bacterial pathway for siderophore biosynthesis independent of nonribosomal peptide synthetases. Chembiochem **6:**601-611.
19. **Chambers, H. F.** 2003. Solving staphylococcal resistance to beta-lactams. Trends Microbiol. **11:**145-148.
20. **Chambers, H. F. and F. R. Deleo.** 2009. Waves of resistance: *Staphylococcus aureus* in the antibiotic era. Nat. Rev. Microbiol. **7:**629-641.
21. **Cheung, A. L., M. G. Bayer, and J. H. Heinrichs.** 1997. *sar* genetic determinants necessary for transcription of RNAII and RNAIII in the *agr* locus of *Staphylococcus aureus*. J. Bacteriol. **179:**3963-3971.
22. **Cheung, A. L., A. S. Bayer, G. Zhang, H. Gresham, and Y. Q. Xiong.** 2004. Regulation of virulence determinants in vitro and in vivo in *Staphylococcus aureus*. FEMS Immunol. Med. Microbiol. **40:**1-9.
23. **Cheung, J., F. C. Beasley, S. Liu, G. A. Lajoie, and D. E. Heinrichs.** 2009. Molecular characterization of staphyloferrin B biosynthesis in *Staphylococcus aureus*. Mol. Microbiol. **74:**594-608.
24. **Clarke, T. E., S. Y. Ku, D. R. Dougan, H. J. Vogel, and L. W. Tari.** 2000. The structure of the ferric siderophore binding protein FhuD complexed with gallichrome. Nat. Struct. Biol. **7:**287-291.
25. **Cockayne, A., P. J. Hill, N. B. Powell, K. Bishop, C. Sims, and P. Williams.** 1998. Molecular cloning of a 32-kilodalton lipoprotein component of a novel iron-regulated *Staphylococcus epidermidis* ABC transporter. Infect. Immun. **66:**3767-3774.
26. **Cope, L. D., R. Yogev, U. Muller-Eberhard, and E. J. Hansen.** 1995. A gene cluster involved in the utilization of both free heme and heme:hemopexin by *Haemophilus influenzae* type b. J. Bacteriol. **177:**2644-2653.
27. **Cotton, J. L., J. Tao, and C. J. Balibar.** 2009. Identification and characterization of the *Staphylococcus aureus* gene cluster coding for staphyloferrin A. Biochemistry **48:**1025-1035.
28. **Coulanges, V., P. Andre, O. Ziegler, L. Buchheit, and D. J. Vidon.** 1997. Utilization of iron-catecholamine complexes involving ferric reductase activity in *Listeria monocytogenes*. Infect. Immun. **65:**2778-2785.
29. **Crosa, J. H. and C. T. Walsh.** 2002. Genetics and assembly line enzymology of siderophore biosynthesis in bacteria. Microbiol. Mol. Biol. Rev. **66:**223-249.
30. **Crossley, K. B. and G. Archer.** 1997. The staphylococci in human disease. Churchill Livingstone, New York.
31. Cuiv, P. O., D. Keogh, P. Clarke, and M. O'Connell. 2008. The *hmuUV* henes of *Sinorhizobium meliloti* 2011 encode the permease and ATPase components of an ABC transport system for the utilization of both haem and the hydroxamate siderophores, ferrichrom and ferrioxamine B. Mol Microbiol. **70(5):** 1261-73.

32. **Dale, S. E., M. T. Sebulsky, and D. E. Heinrichs.** 2004. Involvement of SirABC in iron-siderophore import in *Staphylococcus aureus*. J. Bacteriol. **186:**8356-8362.
33. **Dassa, E. and P. Bouige.** 2001. The ABC of ABCS: a phylogenetic and functional classification of ABC systems in living organisms. Res. Microbiol. **152:**211-229.
34. **de Lorenzo, V. and J. B. Neilands.** 1986. Characterization of iucA and iucC genes of the aerobactin system of plasmid ColV-K30 in *Escherichia coli*. J. Bacteriol. **167:**350-355.
35. **Delany, I., R. Grifantini, E. Bartolini, R. Rappuoli, and V. Scarlato.** 2006. Effect of *Neisseria meningitidis* fur mutations on global control of gene transcription. J. Bacteriol. **188:**2483-2492.
36. **DeLeo, F. R., B. A. Diep, and M. Otto.** 2009. Host defense and pathogenesis in *Staphylococcus aureus* infections. Infect. Dis. Clin. North Am. **23:**17-34.
37. **Deleo, F. R., M. Otto, B. N. Kreiswirth, and H. F. Chambers.** 2010. Community-associated meticillin-resistant *Staphylococcus aureus*. Lancet **375:**1557-1568.
38. **Diekema, D. J., M. A. Pfaller, F. J. Schmitz, J. Smayevsky, J. Bell, R. N. Jones, M. Beach, and SENTRY Partcipants Group.** 2001. Survey of infections due to Staphylococcus species: frequency of occurrence and antimicrobial susceptibility of isolates collected in the United States, Canada, Latin America, Europe, and the Western Pacific region for the SENTRY Antimicrobial Surveillance Program, 1997-1999. Clin. Infect. Dis. **32 Suppl 2:**S114-32.
39. **Doeven, M. K., J. Kok, and B. Poolman.** 2005. Specificity and selectivity determinants of peptide transport in *Lactococcus lactis* and other microorganisms. Mol. Microbiol. **57:**640-649.
40. **Drechsel, H., S. Freund, G. Nicholson, H. Haag, O. Jung, H. Zahner, and G. Jung.** 1993. Purification and chemical characterization of staphyloferrin B, a hydrophilic siderophore from staphylococci. Biometals **6:**185-192.
41. **Dryla, A., D. Gelbmann, A. von Gabain, and E. Nagy.** 2003. Identification of a novel iron regulated staphylococcal surface protein with haptoglobin-haemoglobin binding activity. Mol. Microbiol. **49:**37-53.
42. **Duthie, E. S. and L. L. Lorenz.** 1952. Staphylococcal coagulase; mode of action and antigenicity. J. Gen. Microbiol. **6:**95-107.
43. **Ecker, D. J. and T. Emery.** 1983. Iron uptake from ferrichrome A and iron citrate in *Ustilago sphaerogena*. J. Bacteriol. **155:**616-622.
44. **Emery, T.** 1982. Iron metabolism in humans and plants. Am. Sci. **70:**626-632.
45. **Emery, T. and L. Emery.** 1973. The biological activity of some siderochrome derivatives. Biochem. Biophys. Res. Commun. **50:**670-675.
46. **Evans, S. L., J. E. Arceneaux, B. R. Byers, M. E. Martin, and H. Aranha.** 1986. Ferrous iron transport in *Streptococcus mutans*. J. Bacteriol. **168:**1096-1099.
47. **Fabian, M., E. Solomaha, J. S. Olson, and A. W. Maresso.** 2009. Heme transfer to the bacterial cell envelope occurs via a secreted hemophore in the Gram-positive pathogen *Bacillus anthracis*. J. Biol. Chem. **284:**32138-32146.
48. **Fournier, B. and D. C. Hooper.** 2000. A new two-component regulatory system involved in adhesion, autolysis, and extracellular proteolytic activity of *Staphylococcus aureus*. J. Bacteriol. **182:**3955-3964.

49. **Fournier, B., A. Klier, and G. Rapoport.** 2001. The two-component system ArlS-ArlR is a regulator of virulence gene expression in *Staphylococcus aureus*. Mol. Microbiol. **41:**247-261.
50. **Francis, J. and J. Madinaveitia.** 1949. Isolation from acid-fast bacteria of a growth-factor for *Mycobacterium johnei* and of a precursor of phthiocol. Nature **163:**365.
51. **Gat, O., G. Zaide, I. Inbar, H. Grosfeld, T. Chitlaru, H. Levy, and A. Shafferman.** 2008. Characterization of *Bacillus anthracis* iron-regulated surface determinant (Isd) proteins containing NEAT domains. Mol. Microbiol. **70:**983-999.
52. **Ghigo, J. M., S. Letoffe, and C. Wandersman.** 1997. A new type of hemophore-dependent heme acquisition system of *Serratia marcescens* reconstituted in *Escherichia coli*. J. Bacteriol. **179:**3572-3579.
53. **Giblett, E. R.** 1968. Recent advances in heptoglobin and transferrin genetics. Bibl. Haematol. **29:**10-20.
54. **Gilson, E., C. F. Higgins, M. Hofnung, G. Ferro-Luzzi Ames, and H. Nikaido.** 1982. Extensive homology between membrane-associated components of histidine and maltose transport systems of *Salmonella typhimurium* and *Escherichia coli*. J. Biol. Chem. **257:**9915-9918.
55. **Giraudo, A. T., A. L. Cheung, and R. Nagel.** 1997. The *sae* locus of *Staphylococcus aureus* controls exoprotein synthesis at the transcriptional level. Arch. Microbiol. **168:**53-58.
56. **Giraudo, A. T., A. Calzolari, A. A. Cataldi, C. Bogni, and R. Nagel.** 1999. The *sae* locus of *Staphylococcus aureus* encodes a two-component regulatory system. FEMS Microbiol. Lett. **177:**15-22.
57. **Grigg, J. C., J. Cheung, D. E. Heinrichs, and M. E. Murphy.** 2010. Specificity of Staphyloferrin B recognition by the SirA receptor from *Staphylococcus aureus*. J. Biol. Chem. **285:**34579-34588.
58. **Grigg, J. C., J. D. Cooper, J. Cheung, D. E. Heinrichs, and M. E. Murphy.** 2010. The *Staphylococcus aureus* siderophore receptor HtsA undergoes localized conformational changes to enclose staphyloferrin A in an arginine-rich binding pocket. J. Biol. Chem. **285:**11162-11171.
59. **Guerout-Fleury, A. M., K. Shazand, N. Frandsen, and P. Stragier.** 1995. Antibiotic-resistance cassettes for *Bacillus subtilis*. Gene **167:**335-336.
60. **Haag, H., H. P. Fiedler, J. Meiwes, H. Drechsel, G. Jung, and H. Zahner.** 1994. Isolation and biological characterization of staphyloferrin B, a compound with siderophore activity from staphylococci. FEMS Microbiol. Lett. **115:**125-130.
61. **Hackbarth, C. J. and H. F. Chambers.** 1993. blaI and blaR1 regulate beta-lactamase and PBP 2a production in methicillin-resistant *Staphylococcus aureus*. Antimicrob. Agents Chemother. **37:**1144-1149.
62. **Hantke, K.** 1981. Regulation of ferric iron transport in *Escherichia coli* K12: isolation of a constitutive mutant. Mol. Gen. Genet. **182:**288-292.
63. **Hartleib, J., N. Kohler, R. B. Dickinson, G. S. Chhatwal, J. J. Sixma, O. M. Hartford, T. J. Foster, G. Peters, B. E. Kehrel, and M. Herrmann.** 2000. Protein A is the von Willebrand factor binding protein on *Staphylococcus aureus*. Blood **96:**2149-2156.
64. **Henderson, D. P. and S. M. Payne.** 1994. Characterization of the *Vibrio cholerae* outer membrane heme transport protein HutA: sequence of the gene, regulation of

expression, and homology to the family of TonB-dependent proteins. J. Bacteriol. **176:**3269-3277.
65. **Hider, R. C. and X. Kong.** 2010. Chemistry and biology of siderophores. Nat. Prod. Rep. **27:**637-657.
66. **Hider, R. C. and A. D. Hall.** 1991. Clinically useful chelators of tripositive elements. Prog. Med. Chem. **28:**41-173.
67. **Ho, W. W., H. Li, S. Eakanunkul, Y. Tong, A. Wilks, M. Guo, and T. L. Poulos.** 2007. Holo- and apo-bound structures of bacterial periplasmic heme-binding proteins. J. Biol. Chem. **282:**35796-35802.
68. **Hoegy, F., H. Celia, G. L. Mislin, M. Vincent, J. Gallay, and I. J. Schalk.** 2005. Binding of iron-free siderophore, a common feature of siderophore outer membrane transporters of *Escherichia coli* and *Pseudomonas aeruginosa*. J. Biol. Chem. **280:**20222-20230.
69. **Holden, M. T., E. J. Feil, J. A. Lindsay, S. J. Peacock, N. P. Day, M. C. Enright, T. J. Foster, C. E. Moore, L. Hurst, R. Atkin, A. Barron, N. Bason, S. D. Bentley, C. Chillingworth, T. Chillingworth, C. Churcher, L. Clark, C. Corton, A. Cronin, J. Doggett, L. Dowd, T. Feltwell, Z. Hance, B. Harris, H. Hauser, S. Holroyd, K. Jagels, K. D. James, N. Lennard, A. Line, R. Mayes, S. Moule, K. Mungall, D. Ormond, M. A. Quail, E. Rabbinowitsch, K. Rutherford, M. Sanders, S. Sharp, M. Simmonds, K. Stevens, S. Whitehead, B. G. Barrell, B. G. Spratt, and J. Parkhill.** 2004. Complete genomes of two clinical *Staphylococcus aureus* strains: evidence for the rapid evolution of virulence and drug resistance. Proc. Natl. Acad. Sci. U. S. A. **101:**9786-9791.
70. **Holland, I. B. and M. A. Blight.** 1999. ABC-ATPases, adaptable energy generators fuelling transmembrane movement of a variety of molecules in organisms from bacteria to humans. J. Mol. Biol. **293:**381-399.
71. **Hoy, T. G. and A. Jacobs.** 1981. Ferritin polymers and the formation of haemosiderin. Br. J. Haematol. **49:**593-602.
72. **Huebner, J. and D. A. Goldmann.** 1999. Coagulase-negative staphylococci: role as pathogens. Annu. Rev. Med. **50:**223-236.
73. **Hunt, L. T., W. C. Barker, and H. R. Chen.** 1987. A domain structure common to hemopexin, vitronectin, interstitial collagenase, and a collagenase homolog. Protein Seq. Data Anal. **1:**21-26.
74. **Idei, A., E. Kawai, H. Akatsuka, and K. Omori.** 1999. Cloning and characterization of the *Pseudomonas fluorescens* ATP-binding cassette exporter, HasDEF, for the heme acquisition protein HasA. J. Bacteriol. **181:**7545-7551.
75. **Isied, S. S., G. Kuo, and K. N. Raymond.** 1976. Coordination isomers of biological iron transport compounds. V. The preparation and chirality of the chromium(III) enterobactin complex and model tris(catechol)chromium(III) analogues. J. Am. Chem. Soc. **98:**1763-1767.
76. **Kammler, M., C. Schon, and K. Hantke.** 1993. Characterization of the ferrous iron uptake system of *Escherichia coli*. J. Bacteriol. **175:**6212-6219.
77. **Kaplan, S. L.** 2005. Implications of methicillin-resistant Staphylococcus aureus as a community-acquired pathogen in pediatric patients. Infect. Dis. Clin. North Am. **19:**747-757.

78. **Karpowich, N. K., H. H. Huang, P. C. Smith, and J. F. Hunt.** 2003. Crystal structures of the BtuF periplasmic-binding protein for vitamin B12 suggest a functionally important reduction in protein mobility upon ligand binding. J. Biol. Chem. **278:**8429-8434.
79. **Klevens, R. M., M. A. Morrison, J. Nadle, S. Petit, K. Gershman, S. Ray, L. H. Harrison, R. Lynfield, G. Dumyati, J. M. Townes, A. S. Craig, E. R. Zell, G. E. Fosheim, L. K. McDougal, R. B. Carey, S. K. Fridkin, and Active Bacterial Core surveillance (ABCs) MRSA Investigators.** 2007. Invasive methicillin-resistant *Staphylococcus aureus* infections in the United States. JAMA **298:**1763-1771.
80. **Konetschny-Rapp, S., G. Jung, J. Meiwes, and H. Zahner.** 1990. Staphyloferrin A: a structurally new siderophore from staphylococci. Eur. J. Biochem. **191:**65-74.
81. **Kreiswirth, B. N., S. Lofdahl, M. J. Betley, M. O'Reilly, P. M. Schlievert, M. S. Bergdoll, and R. P. Novick.** 1983. The toxic shock syndrome exotoxin structural gene is not detectably transmitted by a prophage. Nature **305:**709-712.
82. **Krewulak, K. D., C. M. Shepherd, and H. J. Vogel.** 2005. Molecular dynamics simulations of the periplasmic ferric-hydroxamate binding protein FhuD. Biometals **18:**375-386.
83. **Kristiansen, M., J. H. Graversen, C. Jacobsen, O. Sonne, H. J. Hoffman, S. K. Law, and S. K. Moestrup.** 2001. Identification of the haemoglobin scavenger receptor. Nature **409:**198-201.
84. **Lee, C. Y. and J. J. Iandolo.** 1986. Lysogenic conversion of staphylococcal lipase is caused by insertion of the bacteriophage L54a genome into the lipase structural gene. J. Bacteriol. **166:**385-391.
85. **Lee, J. Y., B. K. Janes, K. D. Passalacqua, B. F. Pfleger, N. H. Bergman, H. Liu, K. Hakansson, R. V. Somu, C. C. Aldrich, S. Cendrowski, P. C. Hanna, and D. H. Sherman.** 2007. Biosynthetic analysis of the petrobactin siderophore pathway from *Bacillus anthracis*. J. Bacteriol. **189:**1698-1710.
86. **Lee, Y. H., R. K. Deka, M. V. Norgard, J. D. Radolf, and C. A. Hasemann.** 1999. *Treponema pallidum* TroA is a periplasmic zinc-binding protein with a helical backbone. Nat. Struct. Biol. **6:**628-633.
87. **Lee, Y. H., M. R. Dorwart, K. R. Hazlett, R. K. Deka, M. V. Norgard, J. D. Radolf, and C. A. Hasemann.** 2002. The crystal structure of Zn(II)-free *Treponema pallidum* TroA, a periplasmic metal-binding protein, reveals a closed conformation. J. Bacteriol. **184:**2300-2304.
88. **Lessard, I. A. and C. T. Walsh.** 1999. VanX, a bacterial D-alanyl-D-alanine dipeptidase: resistance, immunity, or survival function? Proc. Natl. Acad. Sci. U. S. A. **96:**11028-11032.
89. **Lessard, I. A., V. L. Healy, I. S. Park, and C. T. Walsh.** 1999. Determinants for differential effects on D-Ala-D-lactate vs D-Ala-D-Ala formation by the VanA ligase from vancomycin-resistant enterococci. Biochemistry **38:**14006-14022.
90. **Letendre, E. D. and B. E. Holbein.** 1984. Mechanism of impaired iron release by the reticuloendothelial system during the hypoferremic phase of experimental *Neisseria meningitidis* infection in mice. Infect. Immun. **44:**320-325.
91. **Letoffe, S., V. Redeker, and C. Wandersman.** 1998. Isolation and characterization of an extracellular haem-binding protein from *Pseudomonas aeruginosa* that shares

function and sequence similarities with the *Serratia marcescens* HasA haemophore. Mol. Microbiol. **28:**1223-1234.
92. **Lewis, L. A., M. H. Sung, M. Gipson, K. Hartman, and D. W. Dyer.** 1998. Transport of intact porphyrin by HpuAB, the hemoglobin-haptoglobin utilization system of *Neisseria meningitidis*. J. Bacteriol. **180:**6043-6047.
93. **Lewis, L. A., E. Gray, Y. P. Wang, B. A. Roe, and D. W. Dyer.** 1997. Molecular characterization of *hpuAB*, the haemoglobin-haptoglobin-utilization operon of *Neisseria meningitidis*. Mol. Microbiol. **23:**737-749.
94. **Lewis, L. A., M. Gipson, K. Hartman, T. Ownbey, J. Vaughn, and D. W. Dyer.** 1999. Phase variation of HpuAB and HmbR, two distinct haemoglobin receptors of *Neisseria meningitidis* DNM2. Mol. Microbiol. **32:**977-989.
95. **Lindsay, J. A. and M. T. Holden.** 2004. *Staphylococcus aureus*: superbug, super genome? Trends Microbiol. **12:**378-385.
96. **Lindsay, J. A., T. V. Riley, and B. J. Mee.** 1994. Production of siderophore by coagulase-negative staphylococci and its relation to virulence. Eur. J. Clin. Microbiol. Infect. Dis. **13:**1063-1066.
97. **Liu, S., C. Zhang, J. L. Campbell, H. Zhang, K. K. Yeung, V. K. Han, and G. A. Lajoie.** 2005. Formation of phosphopeptide-metal ion complexes in liquid chromatography/electrospray mass spectrometry and their influence on phosphopeptide detection. Rapid Commun. Mass Spectrom. **19:**2747-2756.
98. **Masse, E. and S. Gottesman.** 2002. A small RNA regulates the expression of genes involved in iron metabolism in *Escherichia coli*. Proc. Natl. Acad. Sci. U. S. A. **99:**4620-4625.
99. **Mazmanian, S. K., E. P. Skaar, A. H. Gaspar, M. Humayun, P. Gornicki, J. Jelenska, A. Joachmiak, D. M. Missiakas, and O. Schneewind.** 2003. Passage of heme-iron across the envelope of *Staphylococcus aureus*. Science **299:**906-909.
100. **Meiwes, J., H. P. Fiedler, H. Haag, H. Zahner, S. Konetschny-Rapp, and G. Jung.** 1990. Isolation and characterization of staphyloferrin A, a compound with siderophore activity from *Staphylococcus hyicus* DSM 20459. FEMS Microbiol. Lett. **55:**201-205.
101. **Miller, Y. I. and N. Shaklai.** 1999. Kinetics of hemin distribution in plasma reveals its role in lipoprotein oxidation. Biochim. Biophys. Acta **1454:**153-164.
102. **Mills, S. D., A. Boland, M. P. Sory, P. van der Smissen, C. Kerbourch, B. B. Finlay, and G. R. Cornelis.** 1997. *Yersinia enterocolitica* induces apoptosis in macrophages by a process requiring functional type III secretion and translocation mechanisms and involving YopP, presumably acting as an effector protein. Proc. Natl. Acad. Sci. U. S. A. **94:**12638-12643.
103. **Modun, B., R. W. Evans, C. L. Joannou, and P. Williams.** 1998. Receptor-mediated recognition and uptake of iron from human transferrin by *Staphylococcus aureus* and *Staphylococcus epidermidis*. Infect. Immun. **66:**3591-3596.
104. **Morgan, J. W. and E. Anders.** 1980. Chemical composition of Earth, Venus, and Mercury. Proc. Natl. Acad. Sci. U. S. A. **77:**6973-6977.
105. **Murray, P. R., K. S. Rosenthal, and M. A. Pfaller.** 2009. Medical microbiology. Mosby/Elsevier, Philadelphia.

106. **Muryoi, N., M. T. Tiedemann, M. Pluym, J. Cheung, D. E. Heinrichs, and M. J. Stillman.** 2008. Demonstration of the iron-regulated surface determinant (Isd) heme transfer pathway in *Staphylococcus aureus*. J. Biol. Chem. **283:**28125-28136.
107. **Novick, R. P.** 2003. Autoinduction and signal transduction in the regulation of staphylococcal virulence. Mol. Microbiol. **48:**1429-1449.
108. **Ochsner, U. A., Z. Johnson, and M. L. Vasil.** 2000. Genetics and regulation of two distinct haem-uptake systems, *phu* and *has*, in *Pseudomonas aeruginosa*. Microbiology **146 (Pt 1):**185-198.
109. **Otto, B. R., A. M. Verweij-van Vught, and D. M. MacLaren.** 1992. Transferrins and heme-compounds as iron sources for pathogenic bacteria. Crit. Rev. Microbiol. **18:**217-233.
110. **Paquelin, A., J. M. Ghigo, S. Bertin, and C. Wandersman.** 2001. Characterization of HasB, a *Serratia marcescens* TonB-like protein specifically involved in the haemophore-dependent haem acquisition system. Mol. Microbiol. **42:**995-1005.
111. **Patti, J. M., B. L. Allen, M. J. McGavin, and M. Hook.** 1994. MSCRAMM-mediated adherence of microorganisms to host tissues. Annu Rev Microbiol. **48:**585-617.
112. **Peuckert, F., M. Miethke, A. G. Albrecht, L. O. Essen, and M. A. Marahiel.** 2009. Structural basis and stereochemistry of triscatecholate siderophore binding by FeuA. Angew. Chem. Int. Ed Engl. **48:**7924-7927.
113. **Pfleger, B. F., J. Y. Lee, R. V. Somu, C. C. Aldrich, P. C. Hanna, and D. H. Sherman.** 2007. Characterization and analysis of early enzymes for petrobactin biosynthesis in *Bacillus anthracis*. Biochemistry **46:**4147-4157.
114. **Pierre, J. L. and M. Fontecave.** 1999. Iron and activated oxygen species in biology: the basic chemistry. Biometals **12:**195-199.
115. **Ponka, P.** 1999. Cell biology of heme. Am. J. Med. Sci. **318:**241-256.
116. **Posey, J. E. and F. C. Gherardini.** 2000. Lack of a role for iron in the Lyme disease pathogen. Science **288:**1651-1653.
117. **Quentin, Y., G. Fichant, and F. Denizot.** 1999. Inventory, assembly and analysis of *Bacillus subtilis* ABC transport systems. J. Mol. Biol. **287:**467-484.
118. **Ratledge, C.** 2007. Iron metabolism and infection. Food Nutr. Bull. **28:**S515-23.
119. **Raymond, K. N., E. A. Dertz, and S. S. Kim.** 2003. Enterobactin: an archetype for microbial iron transport. Proc. Natl. Acad. Sci. U. S. A. **100:**3584-3588.
120. **Reniere, M. L., V. J. Torres, and E. P. Skaar.** 2007. Intracellular metalloporphyrin metabolism in *Staphylococcus aureus*. Biometals **20:**333-345.
121. **Roberts, C., K. L. Anderson, E. Murphy, S. J. Projan, W. Mounts, B. Hurlburt, M. Smeltzer, R. Overbeek, T. Disz, and P. M. Dunman.** 2006. Characterizing the effect of the *Staphylococcus aureus* virulence factor regulator, SarA, on log-phase mRNA half-lives. J. Bacteriol. **188:**2593-2603.
122. **Rohrback, M. R., S. Paul, and W. Koster.** 1995. *In vivo* reconstitution of an active siderophore transport system by a binding protein derivative lacking a signal sequence. Mol. Gen. Genet. **248:**33-42.
123. **Rosenbach, F. J.** 1884. Mikro-organismen bei den Wund-Infections-Krankheiten des Menschen. J.F. Bergmann, Wiesbaden.
124. **Rossi, M. S., A. Paquelin, J. M. Ghigo, and C. Wandersman.** 2003. Haemophore-mediated signal transduction across the bacterial cell envelope in *Serratia*

marcescens: the inducer and the transported substrate are different molecules. Mol. Microbiol. **48:**1467-1480.
125. **Rossi, M. S., J. D. Fetherston, S. Letoffe, E. Carniel, R. D. Perry, and J. M. Ghigo.** 2001. Identification and characterization of the hemophore-dependent heme acquisition system of *Yersinia pestis*. Infect. Immun. **69:**6707-6717.
126. **Ryan, K. J., C. G. Ray, and J. C. Sherris.** 2010. Sherris medical microbiology. McGraw Hill Medical, New York.
127. **Sambrook, J., E. F. Fritsch, and T. Maniatis.** 1989. Molecular cloning : a laboratory manual. Cold Spring Harbor Laboratory Press, Cold Spring Harbor, N.Y.
128. **Schneider, E. and S. Hunke.** 1998. ATP-binding-cassette (ABC) transport systems: functional and structural aspects of the ATP-hydrolyzing subunits/domains. FEMS Microbiol. Rev. **22:**1-20.
129. **Schofield, C. J., J. E. Baldwin, M. F. Byford, I. Clifton, J. Hajdu, C. Hensgens, and P. Roach.** 1997. Proteins of the penicillin biosynthesis pathway. Curr. Opin. Struct. Biol. **7:**857-864.
130. **Schryvers, A. B.** 1988. Characterization of the human transferrin and lactoferrin receptors in *Haemophilus influenzae*. Mol. Microbiol. **2:**467-472.
131. **Schryvers, A. B. and L. J. Morris.** 1988. Identification and characterization of the human lactoferrin-binding protein from *Neisseria meningitidis*. Infect. Immun. **56:**1144-1149.
132. **Schryvers, A. B. and L. J. Morris.** 1988. Identification and characterization of the transferrin receptor from *Neisseria meningitidis*. Mol. Microbiol. **2:**281-288.
133. **Schwyn, B. and J. B. Neilands.** 1987. Universal chemical assay for the detection and determination of siderophores. Anal. Biochem. **160:**47-56.
134. **Sebulsky, M. T., B. H. Shilton, C. D. Speziali, and D. E. Heinrichs.** 2003. The role of FhuD2 in iron(III)-hydroxamate transport in *Staphylococcus aureus*. Demonstration that FhuD2 binds iron(III)-hydroxamates but with minimal conformational change and implication of mutations on transport. J. Biol. Chem. **278:**49890-49900.
135. **Sebulsky, M. T., C. D. Speziali, B. H. Shilton, D. R. Edgell, and D. E. Heinrichs.** 2004. FhuD1, a ferric hydroxamate-binding lipoprotein in *Staphylococcus aureus*: a case of gene duplication and lateral transfer. J. Biol. Chem. **279:**53152-53159.
136. **Shi, R., A. Proteau, J. Wagner, Q. Cui, E. O. Purisima, A. Matte, and M. Cygler.** 2009. Trapping open and closed forms of FitE: a group III periplasmic binding protein. Proteins **75:**598-609.
137. **Skaar, E. P., M. Humayun, T. Bae, K. L. DeBord, and O. Schneewind.** 2004. Iron-source preference of *Staphylococcus aureus* infections. Science **305:**1626-1628.
138. **Speziali, C. D., S. E. Dale, J. A. Henderson, E. D. Vines, and D. E. Heinrichs.** 2006. Requirement of *Staphylococcus aureus* ATP-binding cassette-ATPase FhuC for iron-restricted growth and evidence that it functions with more than one iron transporter. J. Bacteriol. **188:**2048-2055.
139. **Stojiljkovic, I. and K. Hantke.** 1995. Functional domains of the *Escherichia coli* ferric uptake regulator protein (Fur). Mol. Gen. Genet. **247:**199-205.
140. **Styers, D., D. J. Sheehan, P. Hogan, and D. F. Sahm.** 2006. Laboratory-based surveillance of current antimicrobial resistance patterns and trends among

Staphylococcus aureus: 2005 status in the United States. Ann. Clin. Microbiol. Antimicrob. **5:**2.
141. **Sussmuth, R. D. and W. Wohlleben.** 2004. The biosynthesis of glycopeptide antibiotics--a model for complex, non-ribosomally synthesized, peptidic secondary metabolites. Appl. Microbiol. Biotechnol. **63:**344-350.
142. **Switalski, L. M., J. M. Patti, W. Butcher, A. G. Gristina, P. Speziale, and M. Hook.** 1993. A collagen receptor on *Staphylococcus aureus* strains isolated from patients with septic arthritis mediates adhesion to cartilage. Mol. Microbiol. **7:**99-107.
143. **Thieken, A. and G. Winkelmann.** 1992. Rhizoferrin: a complexone type siderophore of the Mucorales and Entomophthorales (Zygomycetes). FEMS Microbiol. Lett. **73:**37-41.
144. **Thompson, J. M., H. A. Jones, and R. D. Perry.** 1999. Molecular characterization of the hemin uptake locus (*hmu*) from *Yersinia pestis* and analysis of *hmu* mutants for hemin and hemoprotein utilization. Infect. Immun. **67:**3879-3892.
145. **Tong, Y. and M. Guo.** 2009. Bacterial heme-transport proteins and their heme-coordination modes. Arch. Biochem. Biophys. **481:**1-15.
146. **Torres, V. J., A. S. Attia, W. J. Mason, M. I. Hood, B. D. Corbin, F. C. Beasley, K. L. Anderson, D. L. Stauff, W. H. McDonald, L. J. Zimmerman, D. B. Friedman, D. E. Heinrichs, P. M. Dunman, and E. P. Skaar.** 2010. *Staphylococcus aureus fur* regulates the expression of virulence factors that contribute to the pathogenesis of pneumonia. Infect. Immun. **78:**1618-1628.
147. **Vanderpool, C. K. and S. K. Armstrong.** 2001. The *Bordetella bhu* locus is required for heme iron utilization. J. Bacteriol. **183:**4278-4287.
148. **Vuong, C., H. L. Saenz, F. Gotz, and M. Otto.** 2000. Impact of the *agr* quorum-sensing system on adherence to polystyrene in *Staphylococcus aureus*. J. Infect. Dis. **182:**1688-1693.
149. **Wang, S. C., K. H. Lin, J. P. Chern, M. Y. Lu, S. T. Jou, D. T. Lin, and K. S. Lin.** 2003. Severe bacterial infection in transfusion-dependent patients with thalassemia major. Clin. Infect. Dis. **37:**984-988.
150. **Weems, J. J.,Jr.** 2001. The many faces of *Staphylococcus aureus* infection. Recognizing and managing its life-threatening manifestations. Postgrad. Med. **110:**24-6, 29-31, 35-6.
151. **Weigel, L. M., D. B. Clewell, S. R. Gill, N. C. Clark, L. K. McDougal, S. E. Flannagan, J. F. Kolonay, J. Shetty, G. E. Killgore, and F. C. Tenover.** 2003. Genetic analysis of a high-level vancomycin-resistant isolate of *Staphylococcus aureus*. Science **302:**1569-1571.
152. **Wertheim, H. F., D. C. Melles, M. C. Vos, W. van Leeuwen, A. van Belkum, H. A. Verbrugh, and J. L. Nouwen.** 2005. The role of nasal carriage in *Staphylococcus aureus* infections. Lancet Infect. Dis. **5:**751-762.
153. **Yanisch-Perron, C., J. Vieira, and J. Messing.** 1985. Improved M13 phage cloning vectors and host strains: nucleotide sequences of the M13mp18 and pUC19 vectors. Gene **33:**103-119.
154. **Yarwood, J. M., J. K. McCormick, and P. M. Schlievert.** 2001. Identification of a novel two-component regulatory system that acts in global regulation of virulence factors of *Staphylococcus aureus*. J. Bacteriol. **183:**1113-1123.

155. **Zawadzka, A. M., R. J. Abergel, R. Nichiporuk, U. N. Andersen, and K. N. Raymond.** 2009. Siderophore-mediated iron acquisition systems in *Bacillus cereus*: Identification of receptors for anthrax virulence-associated petrobactin. Biochemistry **48:**3645-3657.
156. **Zawadzka, A. M., Y. Kim, N. Maltseva, R. Nichiporuk, Y. Fan, A. Joachimiak, and K. N. Raymond.** 2009. Characterization of a *Bacillus subtilis* transporter for petrobactin, an anthrax stealth siderophore. Proc. Natl. Acad. Sci. U. S. A. **106:**21854-21859.
157. **Zhu, H., M. Liu, and B. Lei.** 2008. The surface protein Shr of *Streptococcus pyogenes* binds heme and transfers it to the streptococcal heme-binding protein Shp. BMC Microbiol. **8:**15.
158. **Zimmermann, L., K. Hantke, and V. Braun.** 1984. Exogenous induction of the iron dicitrate transport system of *Escherichia coli* K-12. J. Bacteriol. **159:**271-277.